POLITECNICO DI TORINO

Commissions of Civil Engineering

Master of Science in Civil Engineering

Development of a new test method for the determination of the coefficient of thermal expansion and contraction of asphalt concrete

Supervisors

Prof. Davide Dalmazzo
Prof. Ezio Santagata

Candidate

Renato Perra

July 2019

SINTESI

Uno dei principali dissesti che interessano le pavimentazioni stradali di tipo flessibile è rappresentato dalla rottura per fessurazione di origine termica causata dalle basse temperature. Per valutare le tensioni indotte dalle variazioni repentine di temperatura è necessario conoscere il coefficiente di contrazione ed espansione termica. Tale caratteristica risulta di difficile determinazione per materiali dal comportamento complesso come i conglomerati bituminosi e attualmente non sono disponibili procedure standardizzate per la sua determinazione mediante prove di laboratorio.

Il seguente lavoro di tesi ha dunque come obiettivo principale quello di sviluppare un metodo di prova per la determinazione del coefficiente di contrazione ed espansione termica dei conglomerati bituminosi. In particolare, la procedura dovrà essere il più efficiente possibile, riducendo al minimo l'intervento dell'operatore e utilizzando strumenti possibilmente già presenti all'interno dei laboratori di materiali stradali. Lo strumento scelto è il reometro rotazionale a taglio comunemente usato per la caratterizzazione reologica dei materiali e più in particolare dei bitumi. Con esso è infatti possibile misurare con grande precisione la temperatura e le variazioni di lunghezza, input necessari per valutare il coefficiente di contrazione ed espansione. Combinando insieme accessori disponibili, normalmente utilizzati in differenti configurazioni, è stato possibile impostare una nuova configurazione strumentale in grado di ospitare e termostatare campioni cilindrici di adeguate dimensioni e misurarne le variazioni di lunghezza.

Utilizzando diversi gradienti termici e intervalli di misurazione, sono stati sviluppati diversi approcci. Il primo approccio prevede la misurazione delle altezze a temperature specifiche solo quando il campione ha raggiunto l'equilibrio termico. Durante i periodi di condizionamento il sistema di misura viene mantenuto all'esterno della cella in modo da ridurre al minimo le possibili dilatazioni termiche. Nell'intervallo di temperatura scelto vengono però misurati solo pochi punti e dunque le informazioni riguardanti le deformazioni del

campione tra una temperatura e l'altra sono ridotte. Inoltre, per garantire l'equilibrio termico, prima di ogni misura occorre attendere un lungo periodo di tempo a temperatura costante, aumentando la durata della prova. Al fine di ridurre i tempi di prova e riuscire ad avere una descrizione delle deformazioni più dettagliata è stata sviluppata un'altra procedura. In questo caso viene utilizzato un gradiente termico costante e le altezze del campione vengono misurate a intervalli ridotti di pochi secondi. Dai risultati sperimentali è stato osservato come il non raggiungimento dell'equilibrio termico consente di avere tempi di prova più brevi ma comporta degli errori di valutazione del coefficiente causati dalla temperatura variabile e non uniforme all'interno del campione stesso. Inoltre, per eseguire misurazioni più frequenti è necessario che il sistema di misurazione sia mantenuto all'interno della cella subendo deformazioni termiche non note a priori, necessitando quindi una correzione dei risultati ottenuti. Cercando di unire i lati positivi ottenuti dalle due procedure è stato sviluppato un terzo protocollo di prova. Il campione viene sottoposto ad un gradiente costante di temperatura misurandone la lunghezza ad intervalli regolari di 12 minuti, mantenendo tra una misurazione e l'altra il sistema di misura all'esterno della cella termica.

I diversi approcci sono stati validati testando materiali di diversa natura con coefficienti di dilatazione termica noti e molto diversi tra loro come acciaio, alluminio e ceramica. In particolare, è stato riscontrato come la prima procedura proposta risulta essere quella che fornisce i migliori risultati. Per valutare la ripetibilità della prova sono stati condotti differenti cicli termici e di misura ottenendo sui campioni di caratteristiche note gli stessi risultati.

Lo stesso programma di prove è stato effettuato su campioni di conglomerato bituminoso, e i risultati ottenuti hanno mostrato come per tale materiale non solo il coefficiente di contrazione termica differisce da quello di espansione, ma la risposta è influenzata dalla storia termica del materiale. In particolare, è stato osservato come ripetendo la prova sullo stesso campione, il coefficiente di contrazione diminuisce progressivamente mentre il coefficiente di espansione tende a crescere. Tale comportamento può essere legato alla natura viscoelastica del materiale e non alla strumentazione, avendo precedentemente verificato la riproducibilità della prova.

A conclusione del lavoro è stata svolta una indagine sperimentale in cui si è applicato il metodo sviluppato. Per una miscela di conglomerato bituminoso di caratteristiche note è stato investigato come il contenuto dei vuoti potesse influenzare i coefficienti di contrazione ed espansione termica. Sono stati dunque realizzati e testati campioni con diverso contenuto di vuoti. Dai risultati ottenuti si è riscontrato che i vuoti influenzano notevolmente i due coefficienti. In maniera più specifica è stato osservato che all'aumentare dei vuoti consegue un aumento dei coefficienti.

ABSTRACT

One of the main failures affecting flexible pavement is low temperatures thermal cracking. To evaluate the tensions induced by sudden temperature variations it is necessary to know the coefficient of contraction and thermal expansion. This characteristic is difficult to determine for materials with complex behavior such as asphalt concrete and currently no standardized procedures are available for its determination by laboratory tests.

The following thesis has therefore the main objective to develop a test method for determining the coefficient of thermal contraction and expansion of asphhalt concrete. More specifically, the procedure must be as efficient as possible, minimizing operator intervention and using tools already present in the road material laboratories. The instrument chosen is the dynamic shear rheometer (DSR) commonly used for the rheological characterization of materials and more particularly bitumens. With DSR is in fact possible to measure temperature and length's variations with great precision, necessary inputs to evaluate the coefficient of contraction and expansion. By combining together available accessories, normally used in different configurations, it was possible to set up a new instrument configuration able to accommodate and thermostat cylindrical samples of adequate size and measure the variations in length.

Appling different gradients and different interval of measurement different apprached are developed. First approach consists to take height's measurements at specific target temperature when specimen reaches thermal equilibrium. During temperature change the measuring system is kept outside the measuring cell so that the measuring system doesn't deform due to thermal changes. In the temperature range chose only few data points are registered providing few information about specimen's deformation. Moreover, to ensure the thermal equilibrium of the specimen resting time at constant temperature are needed resulting in long duration of the test.

In order to have shorter test duration and more detailed information about deformations a new approach was developed. In this case the thermal gradient is kept constant and measurement height are taken every few seconds. From experimental results was observed how not reaching thermal equilibrium will surely short the procedure but errors will be induced in the evaluation of the CTC and CTE since we will have a difference between the surface and core of the specimen. Moreover, to perform frequent measurements requires the measuring system to be in constant contact with the specimen inside the measuring cell and inevitably it will undergo thermal deformation that must be take into account when analyzing the data.

A third approach was developed trying to merge benefits from the two previous approach. The sample undergoes a constant gradient, and height's measurement are performed every 12 minutes. Between two consecutive measurements the measuring system is kept outside the measuring cell to prevent thermal deformations.

Subsequently the different approaches were validated by testing materials of different nature with known thermal expansion coefficients such as aluminum, ceramic and stainless steel. Was observed that the first approach proposed is the one giving best results and comparable with literature values.

To evaluate the repeatability of the procedure a sample of aluminium underwent different thermal cycles showing same values at each cycle. Same procedure was performed on asphalt concrete sample. Not only we observe differences between CTC and CTE, values differ at each different cycle following a trend. More specifically CTC showed the tendency to decrease while CTE values tend to increase. This behavior is linked to the viscoelastic nature of AC since the same procedure performed on an aluminum sample showed the repeatability of the test.

To conclude, a practical application of the method has been proposed for a bituminous mixture of known characteristics. More specifically was investigated if the percentage of voids could affect the CTC and CTE of bituminous mixtures. Different samples with different voids content were realized and tested. Was observed that voids percentage significantly influence CTC and CTE. More specifically they increase as voids content increase.

INDEX

CHAPTER 1
INTRODUCTION

1.1 Background

Flexible pavement is a layered system where better material are used for the top layers since they are in direct contact with the vehicle and have to assure high performance in terms of comfort, safety and durability. Top layer is realized with a composite material composed by aggregates with different size and bitumen. This kind of material is called asphalt concrete.

Asphalt concrete (AC) is known for his viscoelastic nature and his sensitivity to temperature variations that significantly affect its mechanical properties. With temperature change the AC expands or contracts and the amount of deformation is quantified by the coefficient of thermal expansion and the coefficient of thermal contraction. When deformations are restrained stresses arise inside the pavement. When the pavement is expanding, we have compression stresses while when the pavement is contracting tensile stresses will arise. More specifically if contraction stresses are greater than tensile strength the pavement will damage showing transversal cracks that will accelerate the deterioration and the premature failure of the pavement. This deterioration of the pavement in literature is called thermal cracking.

Thermal cracking is one of the most common pavement distress that requires various input data for its prediction, and more specifically a good evaluation of the coefficient of thermal expansion can lead to a better prediction of thermal cracking.

1.2 Scope and Objective of the study

In the previous paragraph was explained how important is to evaluate the coefficient of thermal contraction (CTC) of asphalt concrete since they are crucial input data for the prevision of stresses that arise in the pavement due to thermal change. However, no regulation for the evaluation of this coefficient in asphalt concrete were disposed and many researchers developed various technique in order to evaluate this coefficient.

The scope of this study is to develop a new test method for the determination of the coefficient of thermal contraction and the coefficient of thermal expansion that can be performed eventually with few interventions of the technician using the disposable instrument of the laboratory.

CTC and CTE for their determination require the measurement of two quantities: displacement and temperature. Dynamic shear rheometer (DSR) fulfil the requirements we need; it is indeed able to measure displacement and temperature with great precision. It is also possible to apply and control heating and cooling rate. For these reasons the test method will be implemented using the DSR.

<div align="right">

CHAPTER 2
ASPHALT CONCRETE

</div>

2.1 Flexible pavements

Flexible pavements as depicted in Figure 2.1 are realized with multiple layers. Starting from the top the pavement consists of surface course, base course, subbase course. Top layers are usually realized with better quality material than those placed at the bottom because they are subjected to higher intensity stress. The function of this type of pavement is to transfer the load generated by vehicles to the existing soil dissipating it through the layers.
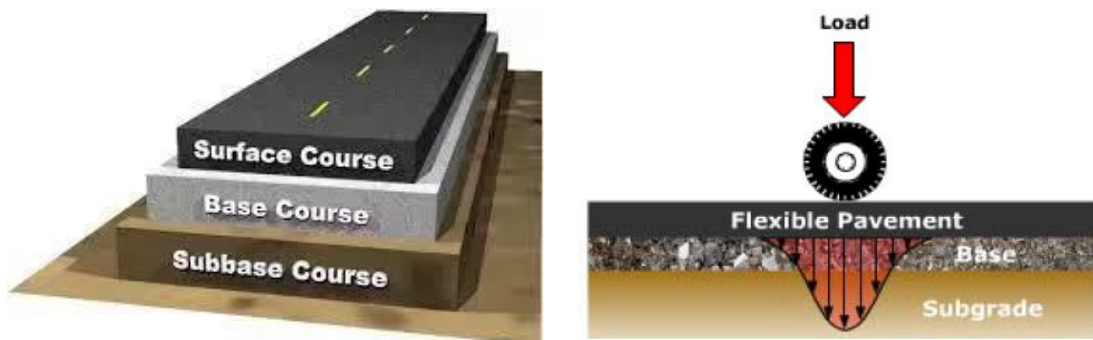
Figure 2.1: Pavement layers (Left) load transfer (right)

The top layer is called surface course and is made of asphalt concrete that is a mixture of bitumen and aggregates of different sizes. The Surface layer can be divided in two different layers itself such as: wearing course and binder course. The wearing course is in direct contact with vehicles it's the one realized with material of the best quality to guarantee best performance. It must be designed to resist distortion under traffic and provide a smooth and skid-resistant surface.

The binder course, placed right under the wearing course, is also made of AC. Presence of a binder course are linked to practical and economic design reasons. AC is indeed too thick to be compacted in a single layer, and in order to have better results in compaction it must be built in different layers. Since lower layers don't require the same quality of the wearing course, the binder is generally realized with larger aggregates and less content of bitumen resulting in a more economic design.

The base course is realized with crushed stone, crushed slag, or other untreated or stabilized materials. The Sub-base course is provided beneath the base course realized with local and cheaper materials.

The Pavement is realized on the existing soil preventively treated. The top 150 mm of the existing soil should be scarified and compacted to the desirable density near the optimum moisture content.

2.2 Asphalt concrete

Asphalt concrete is a composite material with viscoelastic properties largely used for the realization of the surface course of flexible pavement. It's two main materials are bitumen and aggregates that are mixed together following a rational design to obtain best performance possible.

2.2.1 Aggregates

The principal material that constitutes asphalt concrete are aggregates. Aggregates are provided in different sizes and can be classified in three main categories:

- Coarse aggregates
- Mid and Fine aggregates
- Filler

The coarse aggregates give strength to the mix providing interlocking and contact points between aggregates conferring compressive and shear strength to the mix. The mid and fine aggregates fill the voids present between the coarse

aggregates. Fillers particles fills the remaining voids, typical fillers are cement, lime and rock dust.

Based on the size distribution of aggregates inside the mixture we can identify 3 main distribution: Dense graded, gap graded and open graded.

In Figure 2.2 the three kind of distribution are compared and it's already possible to understand their differences.
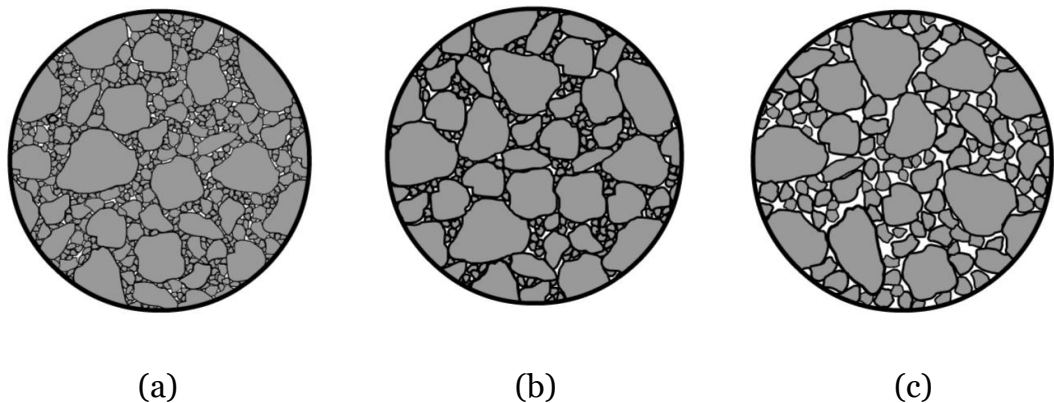

(a)   (b)   (c)

Figure 2.2: Dense graded (a), gap graded (b) and open graded (c)

Dense graded mixture is composed using all sizes of aggregate particles presenting a low percentage of voids. The mixture is characterized by a lot of contact points meaning that load transmission is assured by coarse and finite aggregates.

Gap graded mixture contains few mid aggregates and fine aggregates are only used to fill the gap between coarse aggregate. Stress transmission is ensured by Contact points between coarse aggregates.

Open graded is composed by coarse aggregates and md and few fine particles. This creates a large percentage of voids between the coarse and mid particle size giving to this specific mixture the characteristic of being water permeable.

2.2.2 Bitumen

Bitumen can be found in solid or semi-solid state in nature or more commonly are obtained from oil refining.

Bitumen is the residue of vacuum distillation of oil, consisting of mixtures of hydrocarbons and other complex organic compounds of high molecular weight. Bitumen constitutes is the element that creates cohesion among aggregates of the asphalt concrete, that is largely used for the construction of road and airport pavement.

Bitumen mechanical properties are highly influenced by the temperature. Performing at high temperature it shows typical behaviour of a viscous material while a low temperature its behaviour is more similar to a solid material. The temperature at which this transition starts it called Glass temperature and its definition is very important for practical behaviour.

2.2.3 Mix design

Relationship between weight and volume is important to understand since it gives important information for mix design and construction purposes. Mix design fundamentally consist in determining proportion between bitumen and aggregates in order to obtain a mixture that will satisfy the infrastructure requirement. However, since weight measurements are typically much easier, they are typically taken then converted to volume by using specific gravities.

In Figure 2.3 there's the representation of a typical aggregate distribution where is possible to appreciate how aggregates of different sizes fill the voids present in the volume. It is possible to appreciate that a great amount of the volume is occupied by aggregates the will always leave some voids in between each particle.
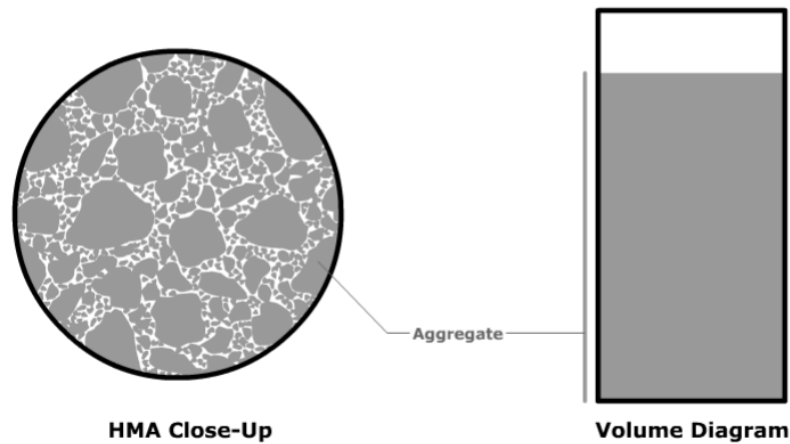
6

Figure 2.3: AC close up (left) volume distribution (right)

In Figure 2.4 it is shown how volume ratio change when bitumen (coloured in black and called asphalt binder) is added to the aggregates. As it possible to appreciate part of volume of the bitumen penetrate the volume of the aggregates. Aggregates surface indeed presents porosity that will absorb part of the bitumen. The amount of bitumen absorbed is called "absorbed asphalt binder" and it doesn't contribute to provide cohesion to the mix. The remaining part of the bitumen, called "effective bitumen", will cover the aggregates creating a bitumen coat and filling parts of the air voids. A certain amount of air voids will be always present in the mix.
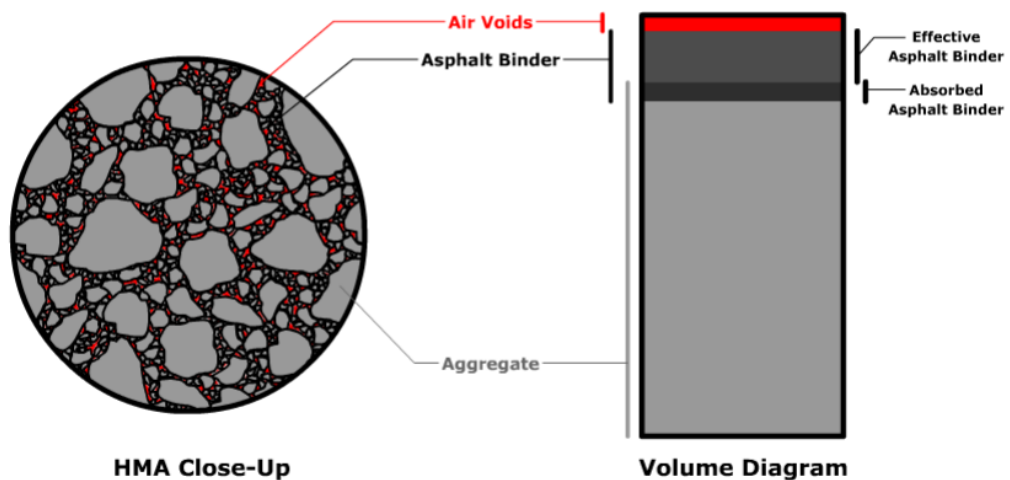

Figure 2.4: AC close up (left) volume distribution (right)

Referring to the volume representation exposed before we can define different relations that describe the volumetric characteristic of the asphalt concrete. The percentage of voids in the mixture is expressed as the ratio between the volume occupied by the air and the volume of the mixture.

$$V_v = \frac{V_a}{V} \cdot 100$$

The volume of intergranular void space between the aggregate particles of an asphalt that consider air voids and the effective bitumen, expressed as a percent of the total volume of the specimen is called voids in mineral aggregates:

$$VMA = \frac{V_a + V_{eff}}{V} \cdot 100$$

Is it also to define the portion of the voids in the mixture that are filled with bitumen as the ratio between the volume of effective bitumen and the volume not occupied by the aggregates.

$$VFA = \frac{V_{eff}}{V_a + V_{eff}} \cdot 100$$

2.2.4 Viscoelastic solutions for asphalt concrete

Asphalt concrete is a viscoelastic material whose behaviour depends from temperature and on the time of loading. A viscoelastic material possesses both the elastic property of a solid and the viscous behaviour of a liquid. The viscous component makes the behaviour of viscoelastic materials time dependent.

To describe the viscoelastic behaviour of the asphalt concrete various mechanical models has been developed combining together two basic elements: a spring (Figure 2.5-left) and a dashpot (Figure 2.5-right).
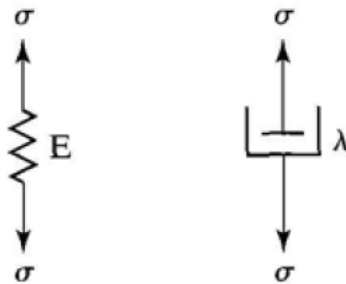

Figure 2.5: Elastic model (left) viscous model (right)

8

Elastic model   The spring is the basic model to characterize an elastic material and it follow Hook's law that express the relationship between stress and strain to be direct proportional.

$$\sigma = E \cdot \varepsilon$$

Where σ is the stress and ε is the strain while E represents the elastic modulus. In Figure 2.6 is shown the strain response under a constant stress. The strain response is immediate as the recovery of deformation as the stress finish.
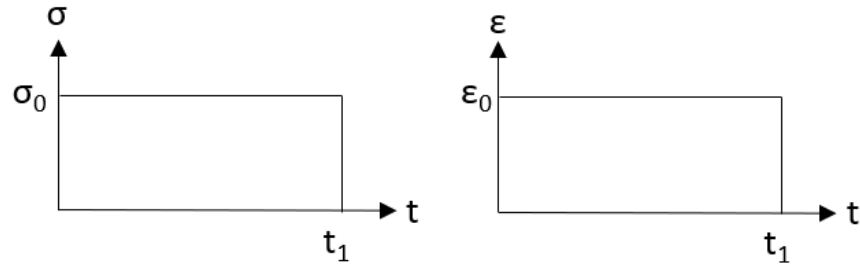

Figure 2.6: Elastic model' strain response (right) due to a constant stress (left)

Viscous model   Viscous material are represented with a dashpot and their behaviour is described by the Newton's law according to which stress is proportional to the time rate of strain:

$$\sigma = \lambda \cdot \frac{\partial \varepsilon}{\partial t}$$

Where σ is the stress and ε is the strain, λ is viscosity and t is time.

In Figure 2.7 is represented the strain response under a constant stress. As stress is applied strain increase following a slope. At the time t_0 when the stress is removed strain is not recovered and we have a permanent deformation.
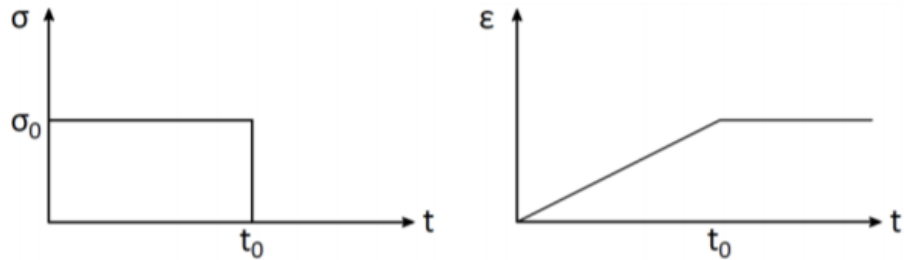

Figure 2.7: Viscous model's strain response (right) due to a constant stress (left)

Maxwell Model   Combining a spring and dashpot in series, as depicted in Figure 2.8 we obtain a Maxwell model.
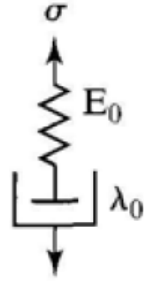
9

Figure 2.8: Maxwell model with spring and dashpot in series

When applying a constant stress, the total strain is the sum of the strains of both spring and dashpot

$$\epsilon = \frac{\sigma}{E_0} + \frac{\sigma \cdot t}{\lambda_0}$$

In Figure 2.9 we observe what happens when this kind of model undergo a constant stress. As the load is applied at t_0 a stress σ_0 will arise. In terms of strain at the time t_0 we have the contribute of the spring the immediately deform and for all the of application of the load we have the contribute of the dashpot that will deform linearly during time. As the load is removed at t_1 the elastic deformation is immediately recovered but after t_1 we will have a permanent deformation due to the dashpot.
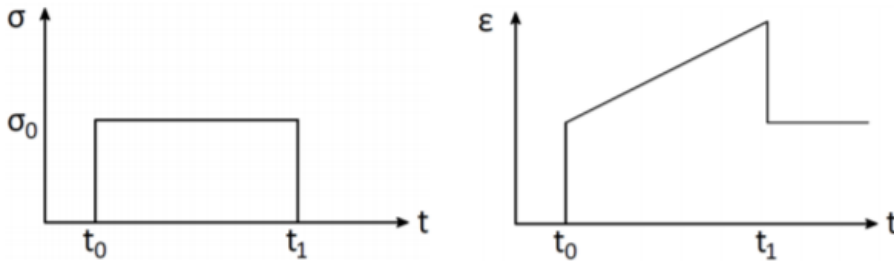
Figure 2.9: Maxwell model' strain response (right) due to a constant stress (left)

Is also interesting to analyse what happens to stress when we apply a constant strain as represented in Figure 2.10. At the time t_0 a constant strain ε_0 is applied and kept constant. At the time t_0 stress immediately arise due to the presence of the spring but in time stress will decrease due to the contribute of the dashpot. Eventually after a time long enough stress will totally disappear.

10
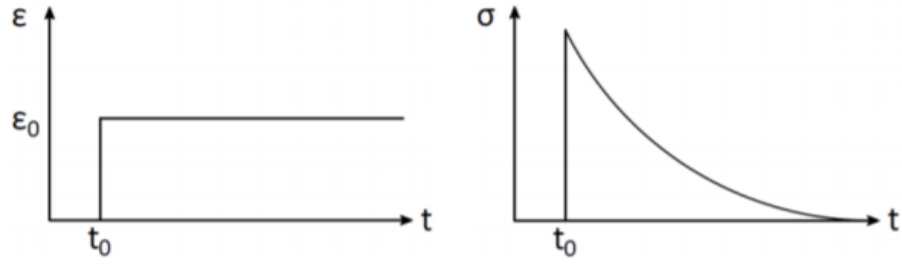
Figure 2.10: Maxwell model's relaxation of stress due to constant strain

Kelvin model   Combining a spring and dashpot in parallel, as depicted in Figure 2.11 we obtain a Kelvin model.
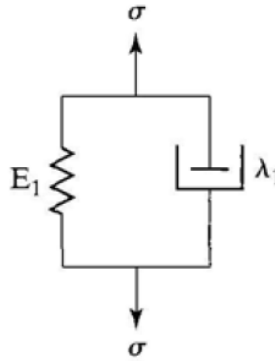
Figure 2.11:Kelvin model with spring and dashpot in parallel

Both the spring and the dashpot have the same strain, but the total stress is the sum of the two stresses.

$$\sigma = E_1 \cdot \varepsilon + \lambda_1 \cdot \frac{\partial \varepsilon}{\partial t}$$

In Figure 2.12 we observe what happens when Kelvin model undergo a constant stress. When at time t_0 a load is applied to the system the σ_0 stress will arise. At the same time the spring tries to stretch immediately but is hold by the dashpot retarding the strain. The system starts to deform with a slope depending on the viscosity of the dashpot. When at the time t_1 the load is removed, the spring tries to contract but again the dashpot holds its deformation spreading it though time.

Eventually after a time long enough strain will be fully recovered and the system will return to its initial position.
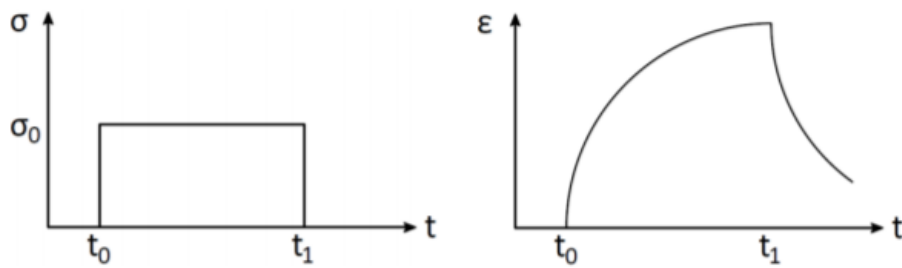
Figure 2.12: Kelvin model' strain response (right) due to a constant stress (left)

2.3 Pavement distresses

When properly designed and maintained asphalt concrete can perform for many years without causing any specific problem. Eventually, some failure may occurs damaging the infrastructure and leading to structural deterioration, loss of the level of comfort and safety. When pavement damage is visible at the surface of the pavement is often called "surface distress" and it is possible to recognize different deterioration of the infrastructure analysing them.

Different manuals are provided in order to identify surface distresses, to evaluate their severity and to repair them. Most common distress to consider flexible pavements are Fatigue cracks, Rutting and thermal cracking. In the following paragraphs a brief description and explanation will be given to the reader.

2.3.1 Fatigue cracks

Fatigue cracks occurs in areas subjected to repeated traffic loadings and unloading that generate inside the pavement alternate tensile and compression stresses as shown in Figure 2.13 leading to a fatigue failure.
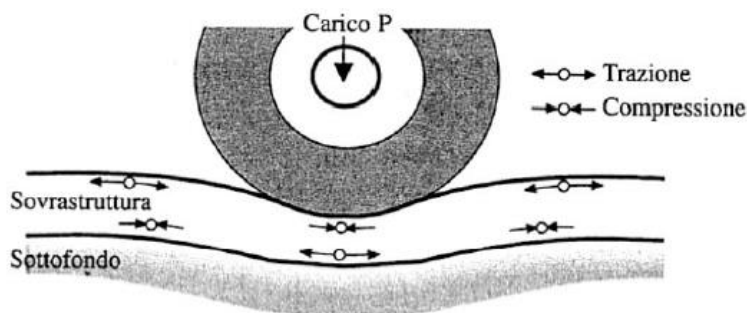
Figure 2.13: Tensile and compression stress in flexible pavement due to traffic loading

Surface distress can be a series of interconnected cracks in early stages of development. Develops into many-sided, sharp angled pieces, usually less than 0.3 m on the longest side, characteristically with a chicken wire/alligator pattern in later stages. In Figure 2.14 are shown typical fatigue cracks of a severe level. In the right picture is possible to appreciate how the distress is localized right under the wheel path.

Figure 2.14: Fatigue cracks of flexible pavement

2.3.2 Rutting

Repetitive loading caused by vehicle together with high temperature and low incorrect compaction of the asphalt concrete leads to permanent deformation in all pavement's layers. This phenomenon generally appears along path wheel as a longitudinal surface depression.

Figure 2.15: Permanent deformation in flexible pavement

2.3.3 Thermal cracks

Especially for pavements that are situated in region characterized by severe low temperature it is common to observe transversal cracks at regular

longitudinal distance. The possible cause of this surface distress is not linked with traffic loading but in this case, it is caused by the environment. Low temperature causes a contraction in the pavement generating this king of distress.

Figure 2.16: Transversal thermal cracks in flexible pavement

2.4 Prediction Model for Thermal Cracking

Thermal Cracking performance Model (TCMODEL) is a mechanics-based developed by National Cooperative Highway Research Program (NCHRP) and implemented in the design guide published by the American Association of State Highway and Transportation Officials (AASHTO). The model predicts the amount of thermal cracking that will develop in a pavement as a function of time.

With low temperature the AC contracts and the amount of deformation is quantified by the coefficient of thermal contraction. In Figure 2.17 is shown the mechanism of thermal cracks. When contraction is restrained tensile stresses arise inside the pavement. If tensile stresses are greater than tensile strength the pavement will damage showing transversal cracks at different points along the length of the pavement [1]. Also, thermal stresses are greatest at the surface of the pavement because pavement temperature is lowest at the surface.
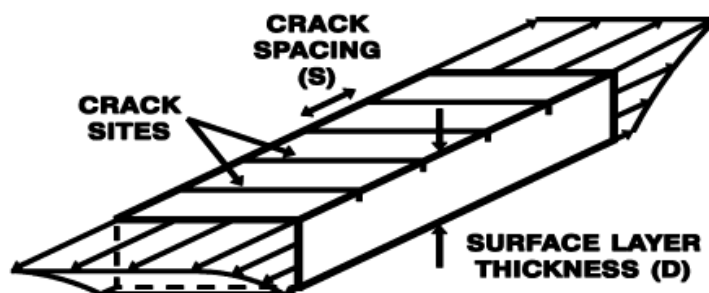
Figure 2.17: Mechanism of thermal cracks in flexible pavement

The input data required for prediction of thermal cracks include pavement structure information, pavement material properties, and site-specific environmental data. More specifically in the section related to material properties the CTC value is needed [1]. To compute the CTC value the guide propose the following relationship that is a modified version of the equation proposed by Jones, Darter, and Littlefield:

$$B_{MIX} = \frac{VMA \cdot B_{AC} + V_{AGG} \cdot B_{AGG}}{3 \cdot V_{TOTAL}}$$

Where:

- B_{MIX} is the linear coefficient of thermal contraction of the asphalt mixture

- B_{AC} is the volumetric coefficient of thermal contraction of the asphalt cement in the solid state

- B_{AGG} volumetric coefficient of thermal contraction of the aggregate

- VMA is the percent volume of voids in the mineral aggregate

- V_{AGG} is the percent volume of aggregate in the mixture

- V_{TOTAL} = 100 percent

The previous relationship to predict the CTC of asphalt concrete considering is mixture characteristic. An accurate prediction of stress in the pavement requires good values of CTC hence specific test must be performed for different asphalt concrete.

<div align="right">

CHAPTER 3
LITERATURE REVIEW

</div>

3.1 Coefficient of Thermal expansion

When a material is subjected to an increase in temperature, we observe it changes in its dimensions. This phenomenon is call thermal expansion and plays an important role in numerous engineering applications. For example, thermal-expansion joints such as those shown in Figure 3.1 must be designed in civil infrastructure, to compensate deformation induced by change in temperature.

<div align="center">(a)   (b)</div>

Figure 3.1: Expansion joint of a bridge (a) and rail (b)

To understand thermal expansion concept from a microscopic point of view let's imagine atoms linked together by springs as shown in Figure 3.2. At room temperature atoms oscillates around their natural position with an amplitude of approximately 10^{-11} m and a frequency of approximately 10^{13} Hz [2]. When temperature increase atoms start oscillating with a bigger amplitude and

as consequence their mutual distance increases causing an expansion of the object considered.
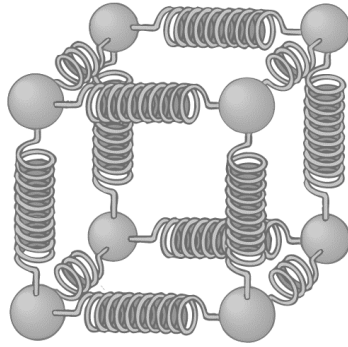
Figure 3.2: 3d disposition of atoms linked with springs

The Coefficient of thermal expansion (CTE) is a material property that is representative of the quantity of expansion of the material upon heating and cooling. Different substances exhibit different amount of expansion. Considering small temperature ranges, the thermal expansion of uniform linear objects is considered to be proportional to temperature change [3]. Different formulae for calculating the coefficient, whether they are expressed referring to a range of temperature or to a specific one, are present in literature.
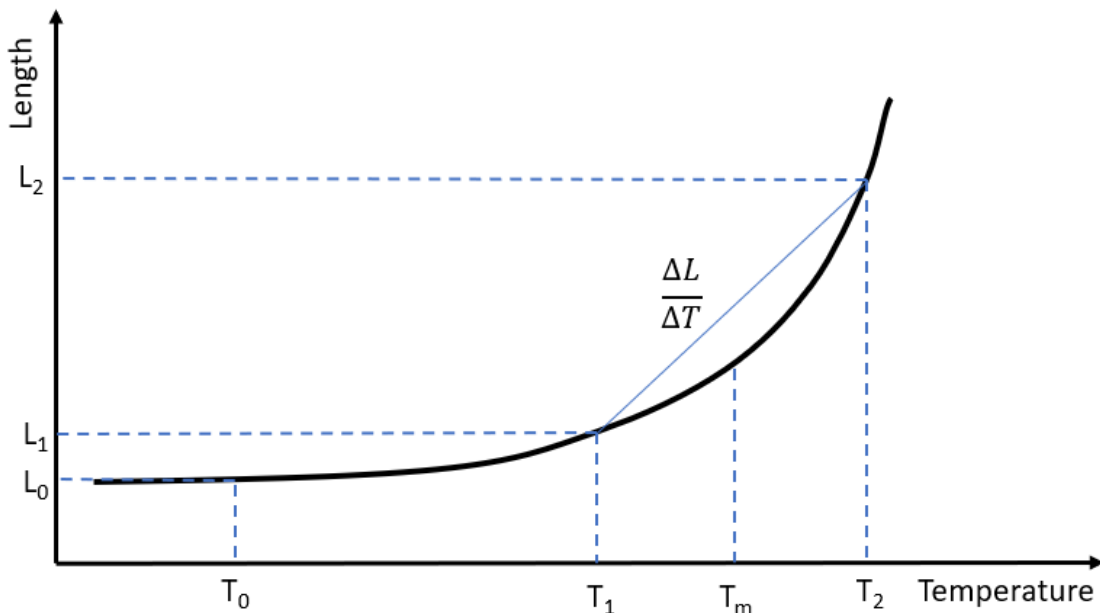
Figure 3.3: Change in length versus change in temperature and α_m slope

The most general definition we can consider the one given by ASM [3]:

$$\alpha_m = \frac{(L_2 - L_1)}{L_0 \cdot (T_2 - T_1)}$$

Here α_m is the average CTE and is referred to the slope of the chord between two point on the curve of length against temperature as shown in Figure 3.3 [4]. This represents the expansion over the specific temperature range from T_1 to T_2. Furthermore, the fractional increase in length is calculated by the increase in length $L_2 - L_1$ by the reference length L_0 measured at T_0. Usually the L_0 is considered the reference length of the object at a reference temperature T_0 that is usually between 20 °C and 30 °C. It is necessary to specify all three temperatures when expressing the value of CTE.

Another way to define CTE over a temperature range is the instantaneous coefficient calculated as follows:

$$\alpha_I = \frac{(L_2 - L_1)}{L_0 \cdot (T_2 - T_1)}$$

The coefficient obtained in this case refers to a specific temperature T_m identified as the average between the two opposite temperature of the range (Figure 3.3):

$$T_m = \frac{(T_1 + T_2)}{2}$$

Alternatively, we can express the true coefficient that is obtained as the slope of the tangent to the curve of length against temperature. The true coefficient can be evaluated as follows:

$$\alpha_t = \frac{1}{L} \cdot \frac{dL}{dT}$$

L in this case is the length considered at the specific temperature we are considering for the evaluation of the true coefficient. This last formula can be seen as the extreme case where the difference between T_1 and T_2 is infinitesimally small.
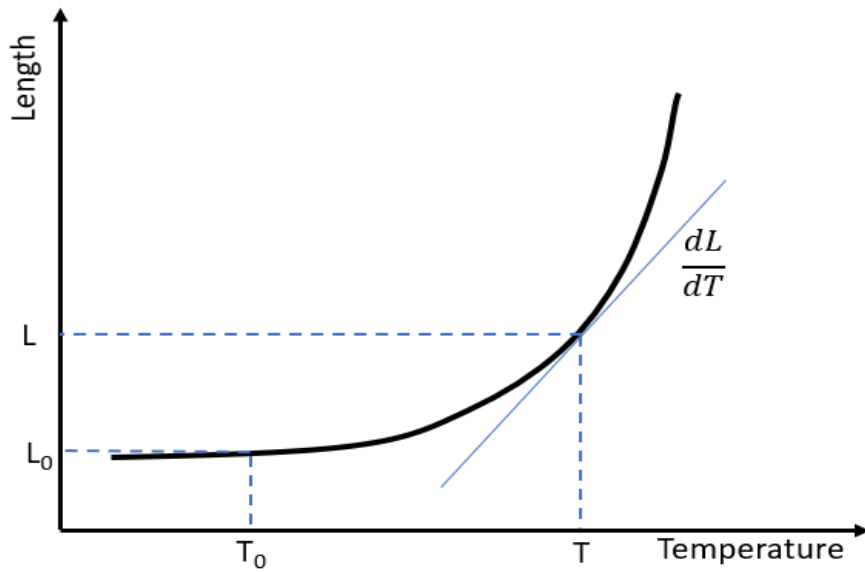
Figure 3.4: Change in length versus change in temperature and α_t slope

However, sometimes for practical reasons it is more convenient to use the original length L_0 measured at room temperature as the denominator for the fractional length change:

$$\alpha_{t*} = \frac{1}{L_0} \cdot \frac{dL}{dT}$$

Since materials expand in all directions due to a change in temperature, similarly to the 1-dimensional case one can express the volumetric expansion coefficient as follows [4]:

$$\alpha_V = \frac{1}{V} \cdot \frac{dV}{dT}$$

- V is the volume measurement of the object

- dV is the change in volume.

- dT is the change in temperature expressed in Celsius or Kelvin.

For isotropic material and small change in dimensions we can relate the linear thermal expansion with volumetric and areal expansion [4]:

$$\alpha_V = 3 \cdot \alpha_L$$

20

3.2 Measurement techniques

To determine the thermal expansion coefficient, displacement and temperature must be measured on a sample that is undergoing a thermal cycle [4]. In the following paragraphs some techniques based on ASTM standards such as push-rod dilatometry [5], thermo mechanical analysis [6] and interferometry [7] will be exposed.

The three methods use an instrumental setup that basically consist in a furnace, which is the device used to control temperature change, and a device that can detect displacements. First two methods transmit change in length with mechanical devices to electronic sensors placed outside the furnace. The third one measures displacement by computing the difference of number of wavelengths generated by a light source and then reflected to a receiver.

3.2.1 Mechanical Dilatometry

Mechanical dilatometry is frequently used for thermal expansion measurement. The displacement of a specimen due to thermal changes is mechanically transmitted to a sensor located away from the heated environment.

The specimen must be between 25 mm and 60 mm long and between 5 mm and 10 mm in diameter or, if its cross section is not cylindrical, must have an equivalent cross section area. As depicted in Figure 3.5 the sample is placed in a furnace where a push rod is in contact with a face of the specimen parallel to the direction of expansion. As the specimen expands the rod will mechanically transmit displacement to displacement sensor such as a linear variable differential transformer (LVDT) placed in a thermally isolated environment at room. Depending on the material of the push rod the temperature range of investigation change. Vitreous silica push rod allows a temperature range from -180 °C and 900 °C while using graphite we can reach temperature up to 2500 °C.
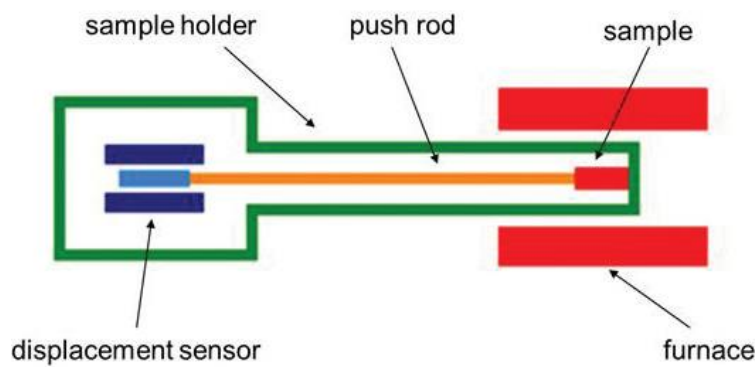
Figure 3.5: Push rod dilatometer configuration

During temperature changes the rod inside the furnace will heat up and expand. To obtain the correct value of CTE/CTC the expansion of the rods must be subtract from the measured change in length. A calibration test must be performed using material with a well known CTE/CTC in order to estimate the expansion and contraction of the rod.

A variation of this technique is the differential dilatometer whose instrumental configuration is reported in Figure 3.6. Two specimens are placed inside the furnace. One of them is made of a reference material of which thermal expansion is well known while the other is the sample to investigate and both are in contact with a push rod that transmit displacement to displacement sensors. The displacement of the tested specimen is obtained as difference from the reference one.
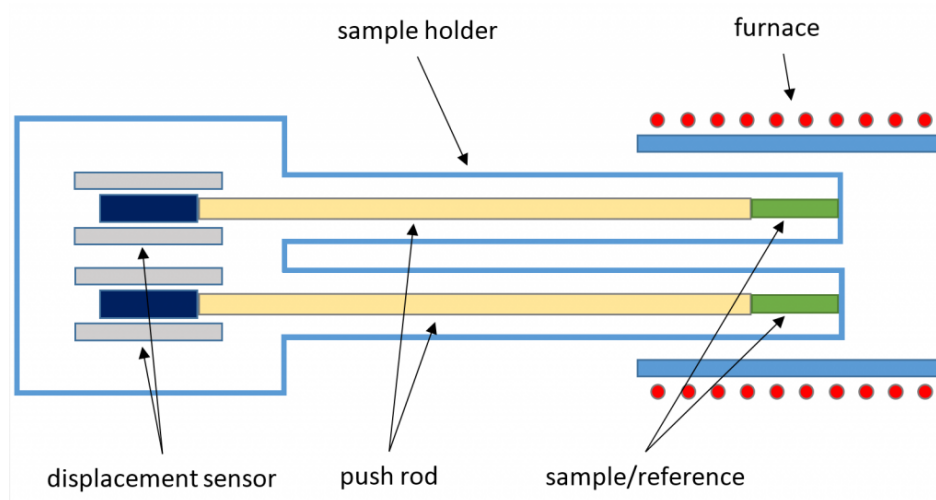
Figure 3.6: Differential push rod dilatometer

3.2.2 Thermo mechanical analysis

Thermo mechanical analysis is a technique that allows to investigate thermal expansion of materials under predetermined force. As represented in Figure 3.7 the sample (green rectangle) is placed on a sample carrier in contact with a quartz push rod that transmit displacement to the displacement transducer. The Push rod can also apply a normal force thanks to an actuator that can perform in static condition or modulating the intensity of the force that is controlled by a force sensor. The range of the force applied suggested is from 0.001 N to 1 N. The Specimen, the probe and the sample carrier are covered with a furnace.
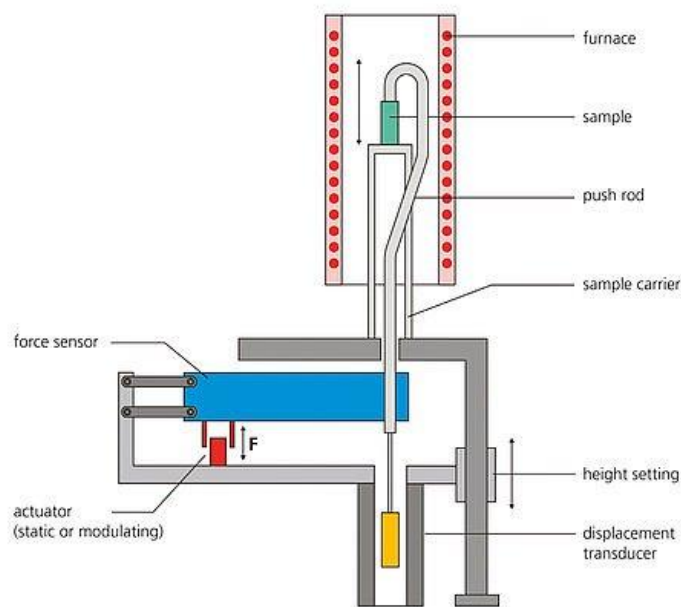
Figure 3.7:Thermo mechanical analyser apparatus

The investigated material should keep properties of a solid material through all the temperature range of investigation in order to prevent any mechanical deformation on the contact area between the specimen and the probe. Temperature range of investigation suggested is from -120 °C and 900 °C but depending on the instrumentation can be extended to higher temperature.

Specimens investigated are very small compared to the push rod dilatometry. ASTM standards suggest that it should have dimension between 2 mm and 10 mm in length and flat parallel ends. Lateral dimensions shouldn't not exceed 10 mm.

3.2.3 Interferometry

The deformation in a specimen under thermal changes can be measured using optical methods. One of this method based on optical interference is the interferometry [5].

A specimen is prepared with polished reflective ends or in can be placed in the middle of two mirrors. The light source usually is a parallel laser beam or from a point monochromatic source that illuminates each surface simultaneously generating a fringe pattern. Expansion or contraction of the specimen causes a change in the fringe pattern because of the difference in the optical pathlength. This change can be computed as difference of number wavelength and converted into length change from which the expansion and expansion coefficient can be determined.

Figure 3.8 is a schematic representation of the single pass Michelson system proposed by ASTM. A light beam usually generated from a laser is split by a beam splitter B. The resulting beams are reflected by mirrors M1 and M'2 and recombined on B. A cylindrical specimen S is placed on one mirror with one face also offered to the incident light. An interference pattern is generated, and this is

split into two fields corresponding to the extremity of the specimen. As the specimen deform, both the specimen and support change of lengths cause the surface S and M'2 to move relative to M1 at different rates. The difference in the fringe count provides a measure of the net absolute expansion.
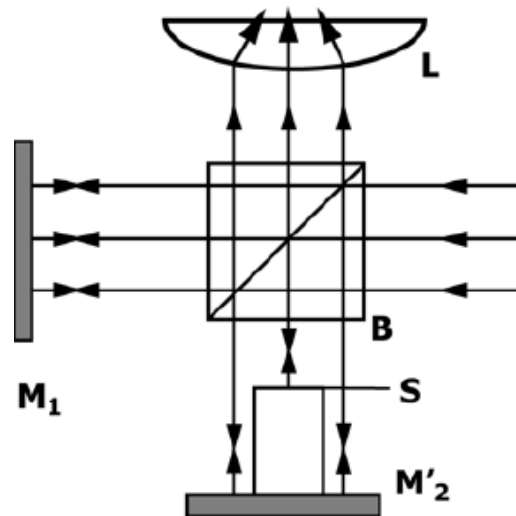
Figure 3.8: Single pass Michelson interferometry system

Figure 3.9 represent the principle of the double pass system very similar to single pass. The interfering beams are reflected twice from each face of the specimen thus giving twice the sensitivity of the single pass, and no reference arm is required.
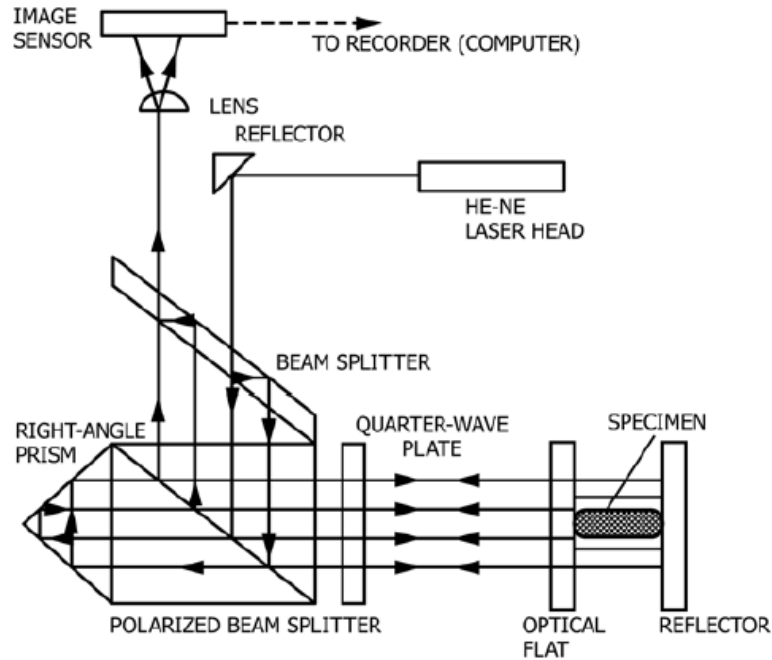
Figure 3.9 : Double pass Michelson interferometry system

The precision of measurement is higher than the two methods discussed before [7]. It is also possible to investigate materials with very low thermal expansion coefficient (below 5 μm/(m·K)). The temperature range at which this test can be performed is from −150°C to 700°C.

3.3 CTE and CTC of asphalt concrete

For solid material deformations induced by a temperature change are the same if we apply a heating ramp or a cooling ramp. In Figure 3.10-a. there's a representation of the deformations caused by a temperature change in a solid material. The blue arrows, that represent deformations during cooling phase, follow the same deformation path (black thick line) as the red arrows that instead represent deformations during the heating phase.

Thermally induced deformation of viscoelastic materials such as asphalt concrete is a more complex matter. In some material the thermal expansion and

contraction can show some discrepancy. After a sudden temperature change, a viscoelastic material may continue to expand or contract in apparent contradiction to the normal response of an elastic material to a temperature change[8]. When cooled or heated asphalt concrete shows differences between CTC and CTE, more specifically was observed that CTC have higher values than CTE [8]–[10]. In terms of deformation this in imply that after a cycle of cooling and heating permanent changes in length are observed.

Figure 3.10 represent the deformation of a viscoelastic material due to temperature change. The blue line represents the evolution of deformations during the cooling phase while the red line represents deformations during heating phase. Comparing these curves with the one for the solid material we notice that curves follow two different paths when going back to the starting temperature (dotted line). A permanent deformation ΔL is observed at the end of the thermal cycle.
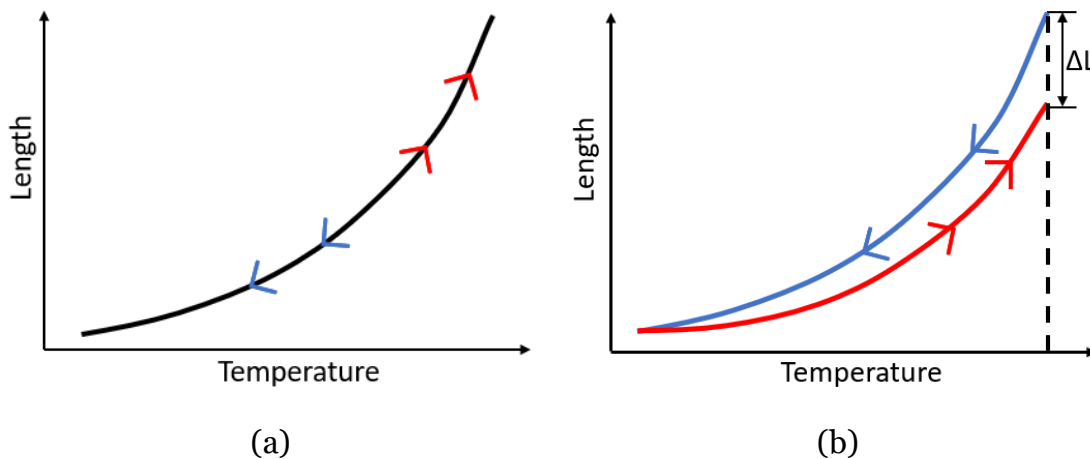
Figure 3.10: Deformation do to temperature change in solid material (a) and viscoelastic material (b)

This phenomenon does not have a specific explanation. One hypothesis is the densification of AC due to irreversible expansion and contraction of the bitumen in the air voids. The effect of gravity force can be another factor that can cause the difference between the two parameters creating resistance during the expansion of the specimen.

CTE and CTC are non-linear function of the temperature and they tend to decrease as the temperature decrease. At low temperature asphalt concrete shows a discontinuity and their value drastically changes. In Viscoelastic theory,

26

considering the relation between deformations and temperature the phase where significative change of trend it's called glass transition and the temperature at which this happens its called glass transition temperature [8]. This transition is important to consider for pavement that perform in country with severe low temperature where it is not so unusual that glass transition temperature lies in the temperature range at which the road is required to perform. Not considering this phenomenon may lead to thermal cracks in the pavement causing relevant distresses and the premature failure of the infrastructure.

Asphalt concrete is a mixture of different material and each one of them if considered alone shows specific thermal characteristics. When mixing them together generate different output in the values of CTC. Some of them tends to have a bigger influence. Different studies focused their attention on this matter changing mixture properties as air voids, binder content, aggregates type and grades [11].

Binder grade was found to have a significant effect on the CTE. More specifically Polymer-modified binder mixtures were found to have a higher CTE compared with neat binder mixtures. Addition of RAP and RAS to asphalt mixtures resulted in a significant reduction in the CTE at relatively colder temperatures. The aggregate CTE had significant effect on the CTE. In fact, aggregates with higher CTE increase the CTE of asphalt mixtures. Aggregate size also affects CTE mixtures, the larger are aggregate sizes the lower are CTEs. Was also found that the amount of bitumen in the mixture is directly proportional with CTE value. The only mixture's characteristic that doesn't show any relevant the air void content [11].

3.4 Measurement techniques for Asphalt concrete

Many researchers have studied different techniques and method to determine CTE and CTC value since this is a very important input data to predict stress in the asphalt concrete and thermal cracking.

Metha et al. [12] measured displacement using linear variable differential transformers (LVDTs). This piece of equipment is normally included in IDT hardware. The method proposed gives slightly more variable values than those

obtained by Stoffles and Kwanda but still comparable. Its effectiveness was evaluated by testing an aluminium beam that was also used to calibrate LVDTs that showed thermal deformation themselves.

Zeng and Shields [8] investigated about the thermal nonlinearity of asphalt concrete. Thermal expansion and contraction were continuously measured on a single type of asphalt concrete in the temperature range from +40°C to −40°C. The specimens used for the tests had a square cross section of 50 mm and 170 mm in length. They found that CTC and CTE were a continuous nonlinear function of temperature and this feature leads to a variable thermal coefficient. However, was found that considering a linear value of CTE and CTC leads to small errors in stress prediction of pavement. The presence of a glass transition is to consider when this lies in the operating temperature. In this case a bi-constant thermal coefficient, one for temperature higher than glass transition and one for temperature lower, is a satisfactory representation of the continuously variable thermal coefficient.

In Figure 3.11 it is depicted the instrumental setup used for the study. The test specimen is placed inside the environmental chamber on a steel support together with a dummy specimen used to understand the temperature distribution inside the test specimen. Test specimen is in contact with two invar rod that transmit displacement to the LVDT placed outside the chamber. Temperature inside the environmental chamber is controlled by mean of a solenoid valve and a fa/ heater is used to homogenize the temperature.
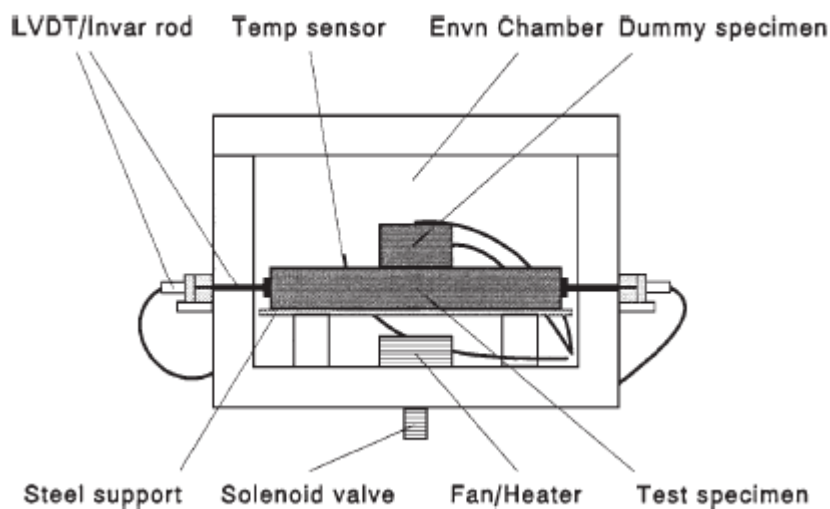

Figure 3.11: Zeng and shield instrumental setup

28

Xu and Solaimanian [13] in their study determined the two coefficients while monitoring the temperature gradient within the material and through the multiple temperature measurements at different depths in a cylindrical specimen. Specimen of ceramic, aluminium and rubber were also tested to validate the method and to calibrate the extensometers. The AC specimens used has cylindrical cross section with a diameter of 100 mm and a height of 150 mm and they were exposed to temperature changes in the range of 40 °C to -5 °C in eight steps. Two different asphalt mixtures were tested. A finite element model was conducted to predict the thermal stress and strain distribution in the specimen caused by temperature change and to determine the location where thermal deformation wasn't restrained. Temperature and strain at this location were then used to calculate the CTE/CTC of AC.

In Figure 3.12 is represented the instrumental setup used. A dual chamber scheme was used to control the testing temperature. Thermocouples were placed on the surface and inserted at different depths in the specimen. Three extensometers with the gage length of 75 mm were mounted on the specimen surface with angular spacing of 120°. These transducers were used to measure the specimen deformations due to temperature changes. The two transducer legs of each extensometer were attached to the specimen surface by two steel wires, and their relative movements were recorded as deformations.
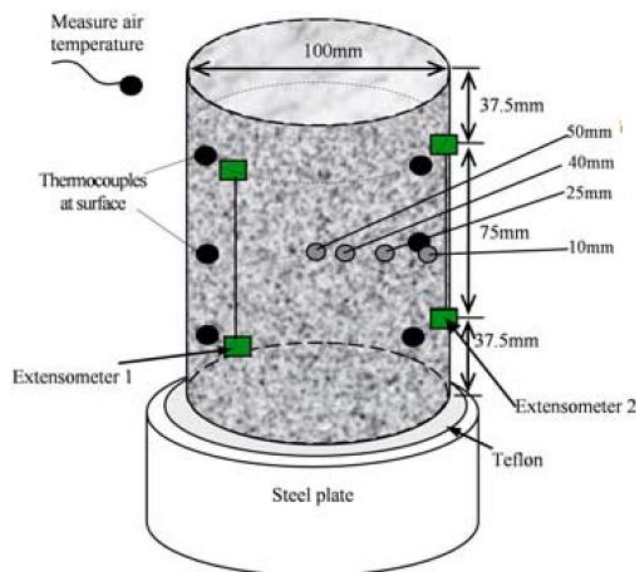

Figure 3.12: Xu and Solaimanian instrumental setup and specimen dimension

Islam and Tarefder [10] conducted a study with the objective to compare CTC and CTE obtained from field data and laboratory data. Field data are obtained installing Horizontal Asphalt Strain Gages in a pavement section located in New Mexico strain, and using these sensors they manage to determine thermal strain variations in fall, winter, and summer. To validate field data CTC and the CTE are measured in the laboratory using three different specimens cored from the pavement section. The three specimens were tested in a temperature range from -10 to 50 °C a displacement was measured using LVDTs and temperature sensors. The LVDTs are calibrated using a cylindrical specimen made by ZERODUR® (Figure 3.13 a), a lithium-aluminosilicate glass-ceramic produced by Schott AG since 1968 characterized by extremely low thermal deformation considered almost equal to zero. Results show that field CTC and CTE values are close to the laboratory findings. Both CTC and CTE are temperature dependent.

Figure 3.13 show the instrumental setup used where the environmental chamber, the same used for dynamic modulus, and LVDT.

(a)   (b)
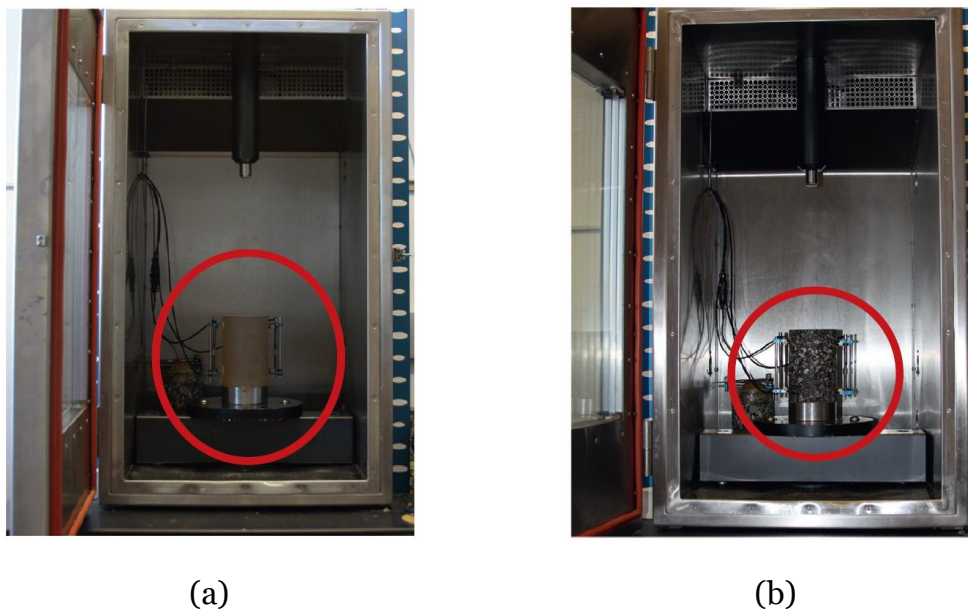
Figure 3.13:Enviromental chamber with ZERODUR® (a) and AC (b), both equipped with LVDTs

Akentuna et al. [11] conducted a study with the purpose to develop new testing device for measuring CTE and CTC easier to run and efficient. Asphalt mixture samples were tested using the Ohio CTE device to determine how mixture properties affect CTE. The asphalt mixture properties investigated under

this study included binder grade, binder content, air void content, aggregate CTE, aggregate size, and mixture aging, as well as the inclusion of recycled asphalt pavements and recycled asphalt shingles.

Figure 3.14 shows the Ohio CTE Device. The frame, realized with aluminium, is placed on its corner on a support. Specimen is placed at the bottom corner of the Ohio CTE device frame during testing. Two LVDTs equipped with flat ends are fixed at the top sides of the device frame in such a way that they are mutually perpendicular and coincide with the diameter of the test specimen. As the temperature changes, the LVDTs take two independent measurements of dimensional change in the test specimen. The change in temperature of the specimen and the frame were measured using four resistance temperature detectors (RTDs) [11].

Figure 3.14: Ohio CTE device with AC sample equipped with resistance temperature

Table 3.1 resume the coefficients of thermal expansion and contraction found in the different investigation exposed above. The second column specify the temperature range at which investigations were conducted. In the third column are expressed CTC and CTE. If not stated, the values expressed are referred only to the CTC since the study was conducted only with cooling ramp.

For asphalt concrete we can observe that CTC values varies from 2.1×10^{-5} and 3.33×10^{-5}. CTE values instead varies between 1.85×10^{-5} and 3.12×10^{-5}. In general, we can observe that CTC has higher values than CTE.

Authors	T range	Thermal coefficient
	°C	°C^{-1}
Littlefield	54 to -18	2.93 - 2.38 x 10^-5
Stoffels and Kawanda	0 to -25	2.97- 1.33 x10^-5
Metha et al	0 to -25	2.94 -1.10 x10^-5
Zeng and Shields	40 to -40	2.63x10^-5 (T>Glass transition)
		1.35x10^-5 (T<Glass transition)
		2.32x10^-5 (average)
Islam and Tarfader	55 to -40	2.57 - 3.33 x 10^-5 (CTC)
		2.63 - 3.12 x 10^-5 (CTE)
Qinwu Xu and Mansour Solaimanian	40 to -4	2.39 - 2.1 x 10^-5 (CTC)
		1.85 - 1.9 x 10^-5 (CTE)

Table 3.1: Coefficients of thermal Expansion and contraction reported in different investigation

CHAPTER 4
DYNAMIC SHEAR RHEOMETER

In order to determine CTC and CTE these two coefficients require the measurement of displacement and a control on the temperature variation. The Dynamic Shear rheometer can perform measure of displacements with a tolerance of 0.001 mm and temperature with a precision of 0.01 °C in the temperature range from -30 °C up to 200 °C applying heating rate up to 8 °C/min and rate up to 4 °C/min. For these specific characteristic dynamic shear rheometer (DSR) was chose to implement the test method for the evaluation of CTC and CTE.

Figure 4.1:Dynamic shear rheometer MCR 302

DSR is normally used for rheology characterization of material and more specifically in our laboratory is mainly used for the characterization of bitumen.

The bitumen sample is placed in the measuring system between two parallel plate (Figure 4.2-a) that can have different diameters or between a plate and a cone (Figure 4.2-b). The upper measuring system is able to rotate and oscillate an generate a torque, hence tests can be conducted applying stress or strain to analyse how bitumen responds in different conditions and so determining its rheologic properties.
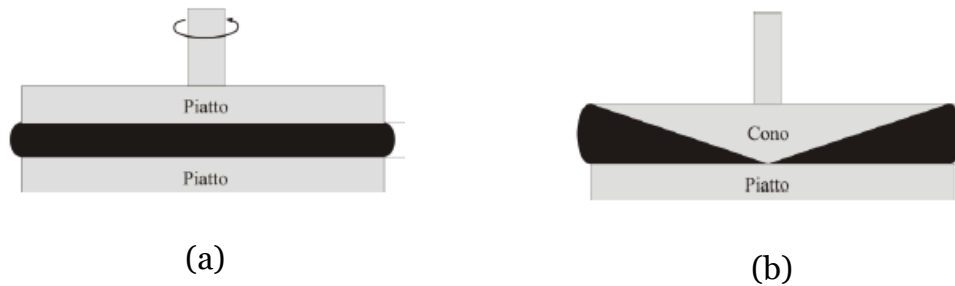

(a)

(b)

Figure 4.2: Plate-plate configuration (a) and plate-cone configuration (b)

The lower measuring system can be changed, and it is possible to use a concentric cylinder instead of a plate configuration creating a new instrumental setup that allow to perform viscosity test on the materials.

The rotor of the EC (Electrically commutated) motor drive is equipped with permanent magnets. In the stator, coils with opposite polarity produce magnetic poles. The magnets in the rotor and the stator coils attract each other, so that a rotating flux of current in the coil windings produces a frictionless synchronous movement of the rotor. Two air bearings systems support the motor: a radial air bearing centres and stabilizes the shaft and the axial air bearing holds the weight of the rotating parts. In the air bearing are integrated normal force sensor. The sensor employs an electric capacity method, precisely converting extremely small deflections in the air bearing into the according normal force. Instead of enforcing additional travel, the natural movement already present in the air bearing is used to measure the normal force.

The temperature is controlled by a Peltier device. Peltier system has two faces, and when a DC electric current flows through the device, it transfers heat from one face to the other. In this way one face of the system gets cooler while the other gets hotter. The hotter face requires a counter cooling so that the cooler face can reach lower temperature.

34

Temperature control device in the configuration Plate-Plate, or Cone-Plate is the P-PTD 200 paired with the hood H-PTD 200 that ensure a homogeneous temperature inside the environment and create a temperature-isolated environment. Figure 4.3 shows a Plate-Plate configuration, and in the scheme on left is it possible to appreciate how the temperature controls works. Peltier device is placed under the measuring plate and in the hood that cover the sample creating a thermal controlled environment.

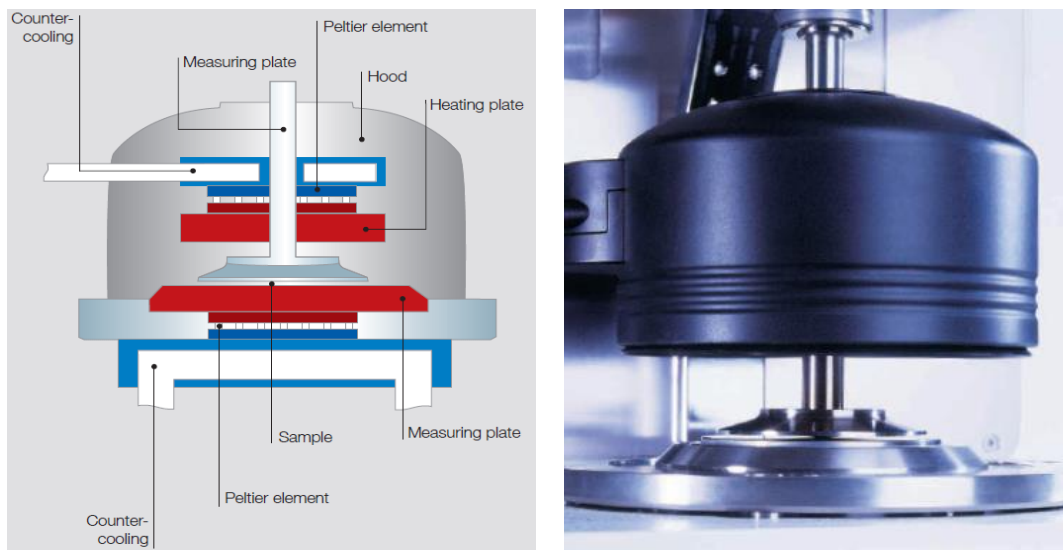
Figure 4.3:P-PTD 200+H-PTD 200 instrumental scheme and setup

In the concentric cylinder configuration, the temperature device used is the C-PTD 200 paired with different cone-spindle. This temperature device, as the P-PTD 200 and the H-PTD 200, uses a Peltier system to control temperature.
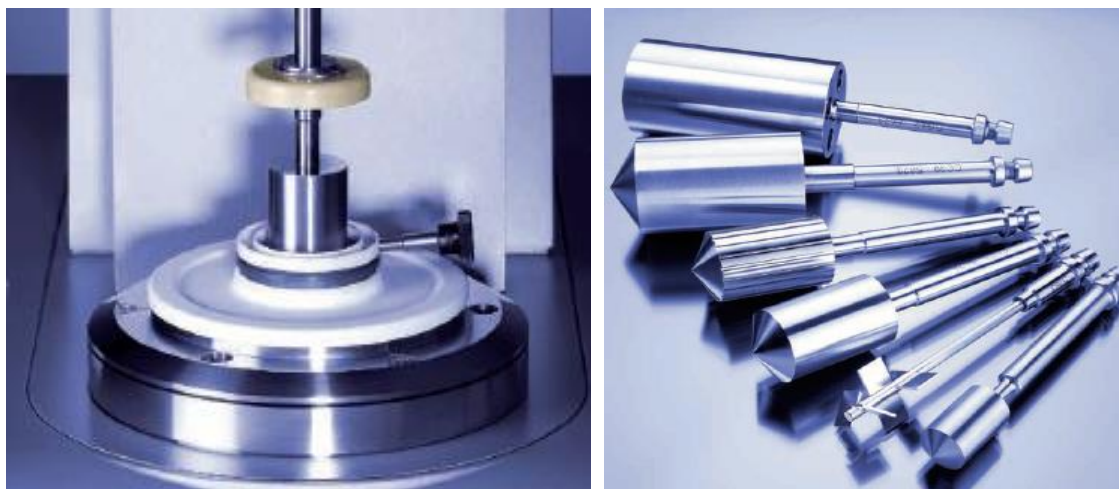
Figure 4.4: C-PTD 200 coupled with cone spindle (left) available spindle for
C- PTD 200 (right)

4.1 Instrumental setup

Using the temperature devices and the measuring system available in the laboratory an instrumental setup had to be studied in order to obtain a good quality of the measurement. The evaluation of CTC and CTE is easier to perform if thermal deformations are big enough and easy to measure. Since the variation of specimen's length is directly proportional to its initial length, the needed instrumental setup had to guarantee an adequately large temperature device in order to accommodate a specimen as large as possible to show great change in length.

The temperature device chose is the C-PTD 200. The device has a depth of 80 mm and cylindrical cross section with a diameter of 40 mm. The operational temperature range is between -30 °C and 200°C and can perform with a heating rate up to 8 °C/min and a cooling rate with 4 °C/min. A H-PTD 200 was used in combination with the C-PTD 200 and placed on the top of it to isolate the environment as shown in Figure 4.5. This hood is a temperature device that perform cooling and heating by convention and helps to keep a homogeneous temperature inside the chamber.
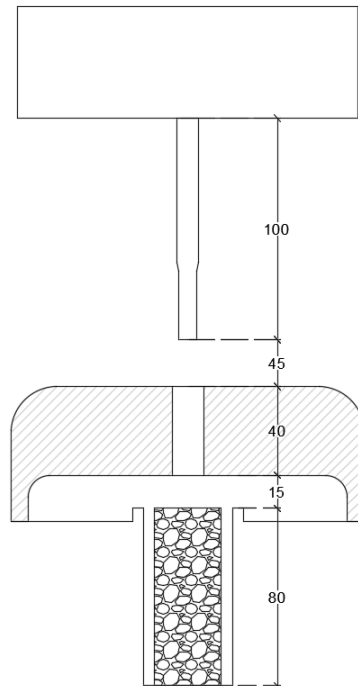
Figure 4.5: Instrumental setup with PP08 and C-PTD 200+H-PTD 200

The measuring system chosen is the plate PP08 with 8 mm of diameter. This measuring system was chosen because it's the only one with a flat surface big enough to generate a good contact with the specimen but also small enough to without any trouble inside the H-PTD 200.

Coupling between measuring system and temperature device are specific. The tool master automatically detects the measuring cell and measuring system and if the two don't match, the whole system locks to prevent damages. In the instrumental setup PP08 and C-PTD 200 are not meant to be coupled together. The measuring system chosen is usually equipped together with a P-PTD 200, while the C-PTD 200 is usually equipped to perform viscosity test. In order to control the temperature device and the measuring system, some setting must be modified. The tool master is disabled, and the detection of the measuring system is made choosing manually the measuring system. As shown in Figure 4.6 we selected the CC28.4 measuring system usually paired with the C-PTD 200.
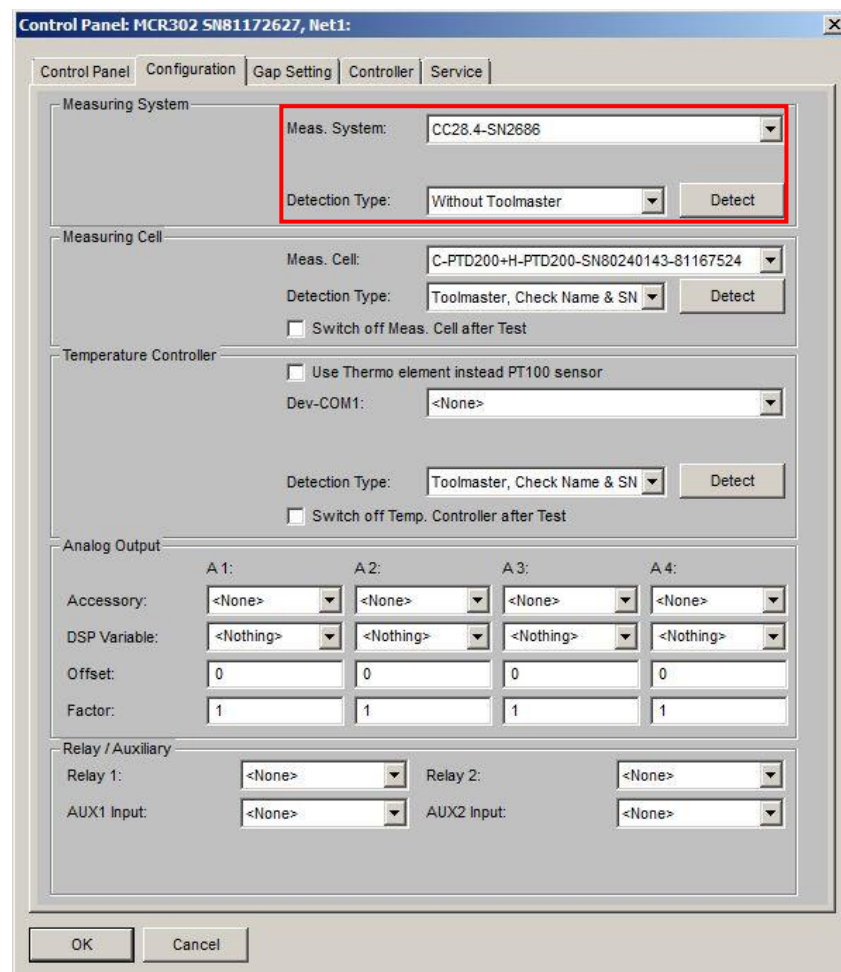
Figure 4.6: Tool master deactivation for measuring system detection

4.2 Gap measurement

In order to obtain a reference point to which gap measurement are referred the instrument need to set a zero gap. Zero gap is set when the contact between the measuring system and the temperature device P-PTD 200 generate a normal force different from zero. The instrumental configuration, due to factory limitation, doesn't allow to set the zero gap and for this reason it's not possible to measure initial length of the specimen but it is still possible to measure the change in length as difference between gap measurement at the two different temperature. The L_0 length used to compute the CTE and CTC is measured with a caliper at the room temperature.

4.2.1 Gapsetting Parameters

In order to understand how the gap is measured a quick explanation a quick explanation about gap parameters and how to control them is needed. The speed of the measuring system and the normal force generated between the measuring system and the specimen are the parameters we need to control to obtain a precise measurement and to prevent any mechanical deformation of the specimen.
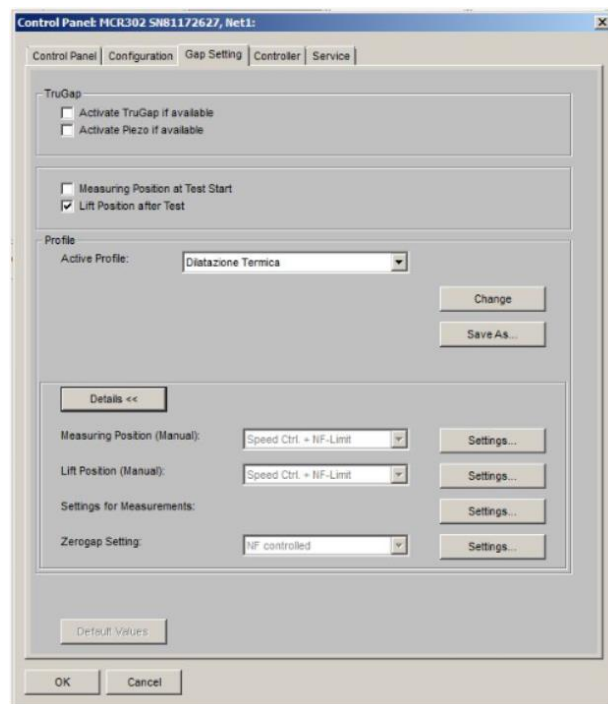
Figure 4.7: Gap setting profile selection

Figure 4.7 shows the gap setting interface. In the bottom part we have to possibility to change the settings for different gap profile. The one needed to control the gap settings during the measurement is called "Settings for measurement".

A profile defines which speed and normal force to use at which position, where position is the vertical position of the measuring System lowest point. The applicability of the test profile limits depends on the selected variable. If normal force or speed are selected as set variables in the measurement profile the values set in the measuring profile will override the values set in this dialog, the limit values are only applied to the variables that are not set.
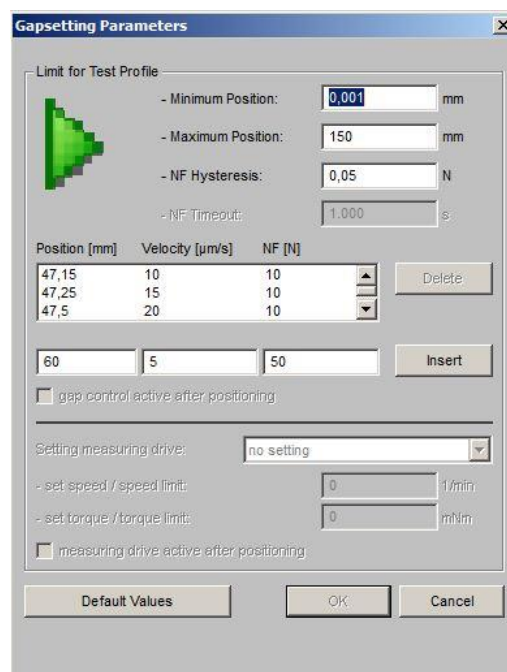
Figure 4.8: Dialog box used for the gapsetting parameters

Figure 4.8 shows the profile used for specimen that has the dimensions discussed before. If dimensions have consistent difference from those specified before then also this profile must be changed. This specific profile guarantee to perform the measurement in the fastest way. Speed are higher far from the specimen and gets slower when reaching the proximity of it.

In Figure 4.8 for example the measuring will proceed at the maximum speed until it reaches a gap equals to 47,5 mm where the speed is changed to 20 µm/s. The speed is constant until gap equals 47,25 mm and the speed is changed to 15 µm/s.

Minimum and maximum position define the range of the gap at which the measuring system is free to move. If the position exceeds these boundaries the DSR will lock to prevent any damage. The 'NF Hysteresis' box defines the allowable deviation of the normal force value from value set in measuring profile before adjusting the normal force again. The 'Position [mm]', 'Velocity [μm/s]' and 'NF [N]' define the speed profile and the maximum force allowable for each position.

4.2.2 Measurement Profile

A measurement profile is a sequence of intervals where is possible to set all parameters for a measurement.

For each interval it is possible to choose the variable measured, the duration of the stage itself and the time between two consecutive measurement. To end an interval before it's time duration it is possible to set an event control where you can establish events and reactions depending on the measured value of a measuring variable or the availability of a measurement result. The event defines the condition that is being checked at every interval of measurement. As soon as the measuring variable match the condition, the reaction will be carried out.

	1 25.000 Pts. 0,1 s	2 30 Pts. 3 s	3 2.000 Pts. 0,1 s	4 50 Pts.
Rotation $\dot{\gamma}$, n , φ , γ	φ 0 mrad	φ 0 mrad	φ 0 mrad	φ 0 mrad
Rotation τ , M				
Oscillation φ , γ				
Oscillation τ , M				
F_N	F_N 0,5 N			
d , v , d/d		v -2 μm/s	v 1 μm/s	d 140 mm
Accessory1 T				

Figure 4.9: Measurement profile used for gap measurement

Figure 4.9 shows the measurement profile used for the gap measurement during the test. Before the test starts the upper plate is in the parking position that is set at 140.00 mm.

The first interval of the measurement profile set as variable the normal force F_N at 0,5 N. As explained in the previous paragraph the speed will be controlled by the Gapsetting Parameters. Therefore, the measurement system will reduce the gap until it reaches a Normal force equals the set value in the measurement profile. To ensure the contact with specimen we need small value of normal force while too high value of normal force will deform the specimen. For this reason, an event control is set to jump to the next step whenever a F_N greater than 0,1 N is measured.

Once contact gap is found, the plate lift with at a constant speed of 2 μm/s (second stage in Figure 4.9). An event control was set to jump forward when the normal force is equal zero.

At this point the measuring system is close enough to the specimen. So, in the third stage (Figure 4.9) the measuring system approach to the sample with a set speed of 1 μm/s and in this case the speed is set by the measurement profile and not by the gapsetting parameters. The speed was set to be the lowest possible in order to guarantee a good measurement of the gap. The event-control set requires moving to the next phase as soon as a normal force greater than 0.1 N is recorded. The data are recorded every 0.1 s to have a detailed description of the event. Only the gap measure that correspond to 0.1 N is considered for the future computation.

Once the third interval finishes, int the fourth interval the measuring system returns to its parking position set at 140 mm.

4.3 Methods development.

A working profile for the measurement of the gap is defined together with an instrumental setup that allows to test specimen with a height of 80 mm and a diameter of 30 mm. Using different combinations of thermal ramp and measurement's interval we can define different methods.

In the first method the specimen's heights are measured only when thermal equilibrium is reached at four specific temperatures. A resting time at the target temperature should be provided to ensure thermal equilibrium through all the specimen's depth.
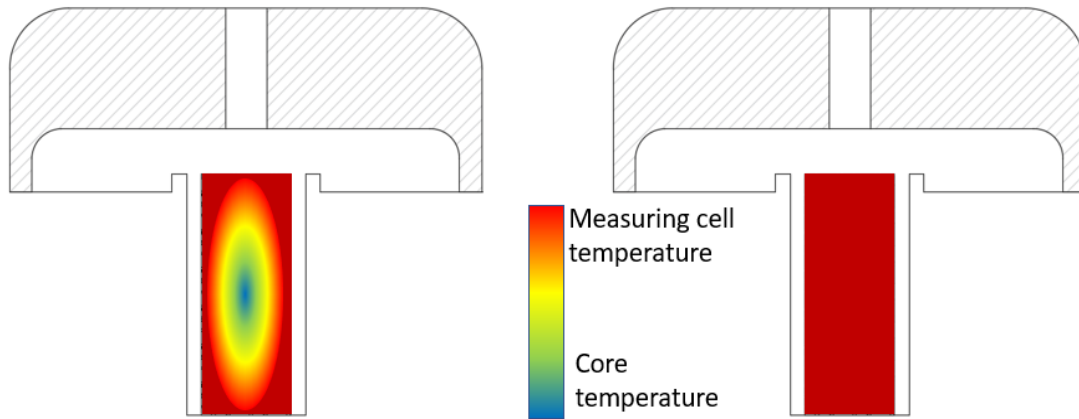
Figure 4.10: Temperature distribution inside AC specimen during thermal ramp (left) and in thermal equilibrium (right)

As depicted in Figure 4.10 on the left side we have the temperature of the surface equals the measuring cell temperature and differs through the depth. This is the situation that happens during the thermal ramp. On the right side of Figure 4.10 we observe that the temperature is the same in all the specimen. The second scenario is the one that happens when the specimen reaches thermal equilibrium.

Figure 4.11 is a qualitative representation of what happens inside the specimen when temperature changes. As the thermal ramp starts the temperature in the measuring cell decreases linearly (blue line), as does the surface temperature of the specimen (orange line) but the specimen's core temperature, due to thermal conductivity and thermal resistance, remains unchanged (transition al phase). Only after a certain time, core's temperature starts to decrease and reach the same thermal gradient of the measuring cell after a transitional phase. This implies that the surface temperature at a certain instant is reached by the core after a time Δt_1. When target temperature is reached (e.g. 20 °C), the measuring cell keeps temperature constant, on the other hand specimen's core has a higher temperature and due to thermal inertia, it needs additional time to reach the target temperature (Δt_2). When measuring cell and core's specimen reaches the same temperature gap measurement can be taken.

At this moment we are sure that stresses caused from the change in the temperature are fully transformed into displacement.
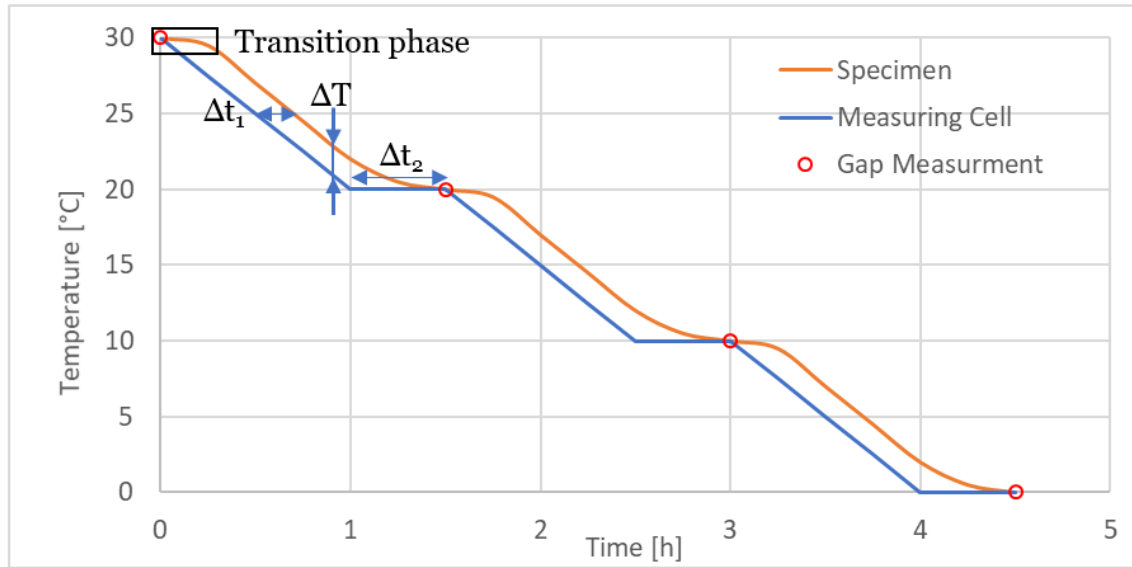
Figure 4.11: Qualitative representation of temperature in measuring cell and in the specimen

To properly set the method, investigations will be conducted to evaluate the time need to reach the thermal equilibrium.

The upper plate, used for the measurement, during the thermal ramp and the resting time is parked outside the measuring cell to avoid any thermal deformation that could induce errors in the measurement. To be sure that the measuring system is not influenced by the air flow coming out from the hood and the concentric cylinder does not deform as well some investigation needs to be conducted.

The method exposed before perform measurement only when thermal equilibrium is reached, and we can evaluate the correct CTC value of the material. but between two consecutive we discussed the test performed in thermal equilibrium. Between two consecutive measurement we don't have any information about specimen deformations. Furthermore, test required long time to be performed. To have a detailed description of the phenomenon we decided to use a constant thermal ramp and maintain contact between the measuring system and the specimen through all the test duration. In this way we can perform measurement with high sampling rate. Performing the test without ensuring thermal equilibrium will induce some errors in the correct evaluation of CTC.

In Figure 4.12 there's a qualitative representation of the temperature profile of specimen (orange line) and measuring cell (blue line) during time. As the thermal ramp starts the temperature in the measuring cell decreases linearly as does the surface temperature of the specimen (blue line), but the specimen's core temperature, due to thermal conductivity and thermal resistance, remains unchanged (orange line). Only after a certain time, core's temperature starts to decrease and reach the same thermal gradient of the measuring cell after a transitional phase. Due to thermal conductivity the temperature change will take some time to reach core's temperature generating a delay ΔT in the temperature profile of the specimen. As temperature change reaches the specimen core's temperature starts changing at the same rate of the measuring cell.

During the thermal ramp the measuring system will undergo temperature changes and inevitably it will deform. This must be considered when computing the CTE since the deformations we will obtain includes asphalt concrete deformations and measuring system deformations. It is necessary to know the thermal expansion and contraction of the measuring system in order to determine the actual deformation of the specimen.
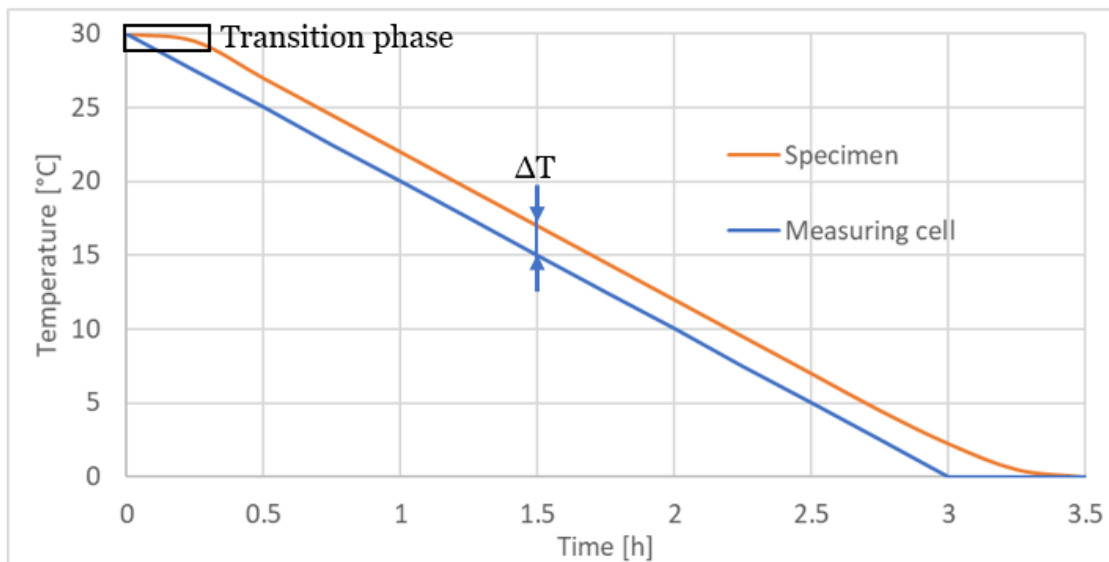
Figure 4.12: Qualitative representation of the temperature trend in the specimen and in the measuring cell.

Based on the previous tests a third method was developed in order to keep the benefits of them. To avoid any uncertainties due to thermal deformation of

the measuring system we want to keep it as much as possible outside of the environmental chamber. A constant thermal ramp is used in order keep the duration of the test as short as possible. Measurements are performed every 12 minutes and between two consecutive measurements the measuring system is kept outside the measuring cell to avoid any thermal deformation.

CHAPTER 5
METHOD DEVELOPMENT

Using different combinations of thermal ramp and measurement's interval, three different methods were developed and tested on an asphalt concrete specimen in the temperature range from 30 °C to -10°C. The specimen has a cylindrical shape with a diameter of 30 mm and a height of 80 mm. These specific dimensions are choose based on studies about the best instrumental setup discussed in Chapter 4.

In the first method the specimen's heights are measured only when thermal equilibrium is reached at four specific temperatures. Every temperature step is made applying a thermal ramp of 10 °C/h after which there's a resting time at the target temperature to ensure thermal equilibrium through all the specimen's depth. The measuring system enters the measuring cell only when the equilibrium is reached.

For the second method a thermal ramp is imposed through all the temperature range chosen with a gradient of 10 °C/h. This imply that specimen never reaches thermal equilibrium and a difference between surface and core's temperature will be always observed causing uncertainties on the evaluation of CTC and CTE. Heights measurements are taken every ten second. For this reason, a constant contact between specimen and measuring system is required and it's ensured by applying a constant normal force of 0.1 N. Since the measuring system undergo temperature's changes it's deformation must be taken into account when evaluating CTC and CTE.

The third method is thought as a combination of the two methods exposed before. The measuring system is kept outside the measuring cell and heights measurement are taken with step of 2 °C without ensuring thermal equilibrium.

5.1 Measurement in thermal equilibrium

To measure the CTC and CTE gap measurement are performed only when specimen's thermal deformations are fully developed meaning that it has reached its thermal equilibrium. In this paragraph the first method developed will be explained.

Before the test stats measurement of the specimen are made at room temperature to determine the L_o dimension. The measurement is made with a caliper.

The specimen is then placed in the measuring cell at the starting temperature of 30 °C for two hours in order to ensure that through the specimen we have a uniform temperature distribution. At this point first measurement is made and this will be the reference measure used to determine the deformation of the specimen. Temperature range chosen is 30 °C to -10 °C and measurement are taken every 10°C. Temperature is changed using a ramp of 10 °C/h and once target temperature is reached the measuring cell keeps the temperature constant until thermal equilibrium is reached.
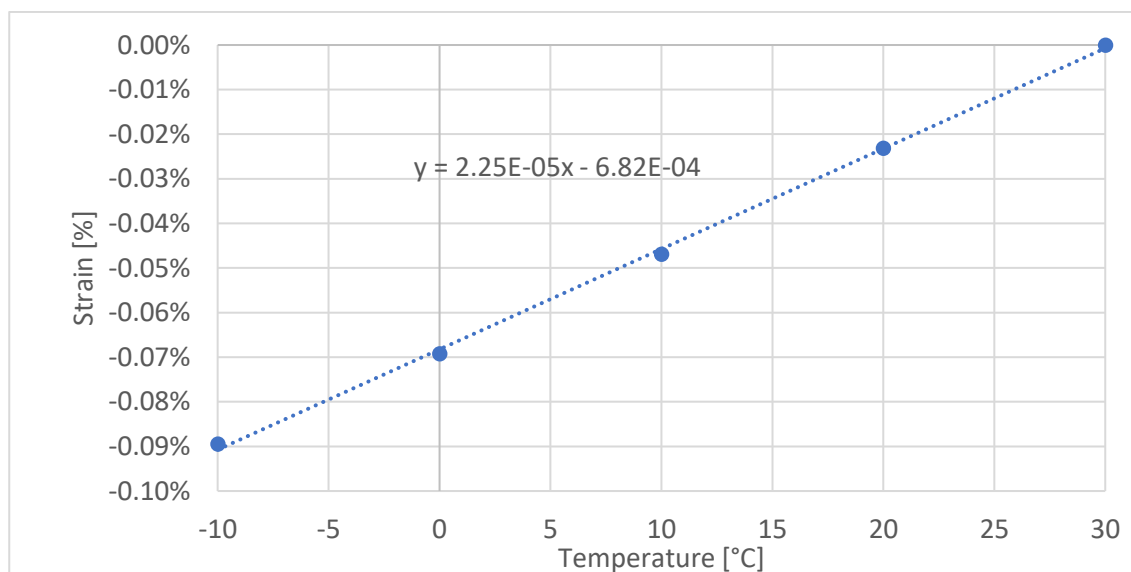

Figure 5.1: Experimental data points with linear regression and its equation

Figure 5.1 represents the gap measurements performed on mixture of asphalt concrete and as we can observe it's CTC is equal to $2.25 \cdot 10^{-5}°C^{-1}$. The CTC obtained it's comparable with those resumed in Table 3.1: Coefficients of thermal Expansion and contraction reported in different investigation.

In the vertical axe we have strain and in the horizontal axe we have the temperature. Strain is computed as:

$$\varepsilon = \frac{\Delta L}{L_0} \cdot 100$$

The CTC is evaluated in the range of 30 to -10 with a linear regression and its value it's equivalent to the slope of it. The method gives the correct value of CTC in the range of temperature considered. To perform this kind of method requires long time, in the range of temperature chosen for example it takes 8 hours, furthermore we have no information how the contraction evolves between two target temperature.

5.1.1 Specimen's thermal equilibrium

When Thermal equilibrium is reached the difference between core temperature and external surface equal zero and all thermal stresses inside the specimen are fully transformed in displacement. This means that to understand when thermal equilibrium is reached, we can observe displacement variation or core's temperature. In the test explained in the previous paragraph the thermal equilibrium is fundamental for the determination of the correct CTC. For this reason, it's important to know the time required the specimen need to reach thermal equilibrium.

Two different investigation were conducted to estimate the minimum time to reach the thermal equilibrium. The first method is based on displacement and consists in measuring every 15 minutes the gap at a constant temperature after a thermal ramp. When gap measurement has a constant value, we can assume that thermal equilibrium is reached. The second method is based on the difference between the measuring cell and core's temperature. A thermometer was drilled into the specimen core and its temperature variation was observed at a constant temperature after a thermal ramp. When core's temperature equals the

measuring cell temperature this was assumed as the moment when thermal equilibrium is reached.

The delay between the time when the measuring cell reaches the target temperature and the thermal equilibrium of the specimen is used to develop the first method.

5.1.1.1 Gap measurement variation

Thermal equilibrium can be identified as the moment in which all the thermal stresses inside the specimen transform into displacement. When this condition happens after a temperature change means that the specimen is in thermal equilibrium. Its length remains constant and so we will have always the same gap measurement.

Before starting the method, the specimen was left for 2 hours at the starting temperature to ensure is thermal equilibrium. A thermal gradient of 10 °C/h was used to change the measuring cell's temperature. Once the target temperature is reached, the gap is measured. The temperature is kept constant and gap measurements are made every 15 minutes. When no gap variation occurs after 3 measurements in a row it's assumed that the specimen has reached the thermal equilibrium. It has been observed that the heart of the sample reaches the target temperature with a delay respect to the measuring cell.

The investigation was performed in cooling and heating ramp. The cooling ramp was performed from 20 to 0°C and heating ramp was performed from 0 to 30 °C.

In Table 5.1 and in Figure 5.2 it is possible to observe the cooling ramp (blue line) from 20 to 0 °C. The measuring cell after 120 minutes is at the target temperature of 20 °C and we can notice that specimen lenght (orange indicators) is contracting but still has not reach the thermal equilibrium because in the succesive gap measuring we can observe that it's still contracting . Thermal equilibrium is reached between 135 and 150 minutes, in fact after 150 minutes we observe three consecutive equal gap messurement. We then assumed that the specimen reached thermal equilibrium with a delay of 30 minutes.

Tempo	T	ΔL
min	°C	[μm]
0	20	0
120	0	-17
135	0	-19
150	0	-20
165	0	-20
180	0	-20

Table 5.1: Investigation of thermal equilibrium in cooling ramp.
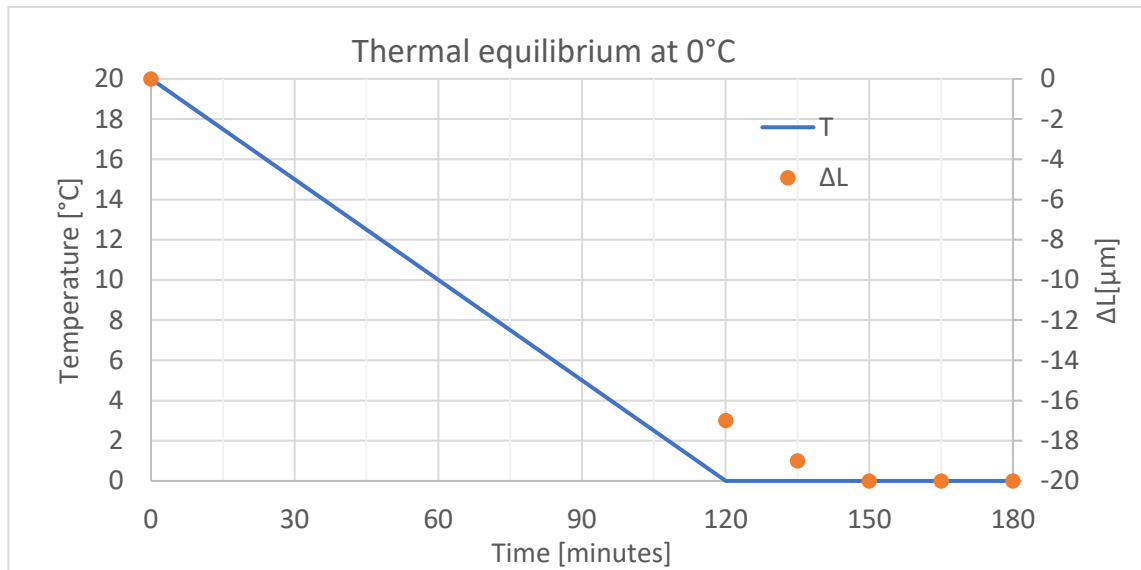
Figure 5.2: Investigation of thermal equilibrium in cooling ramp.

In Table 5.2 and in Figure 5.3 it is possible to observe the heating ramp from 0 to 30 °C (blue line). The measuring cell after 180 minutes is at the target temperature and we can notice that specimen is expanding but still has not reach the thermal equilibrium because in the succesive gap measurement we can observe that it's still expanding . Thermal equilibrium is reached between 210 and 195 minutes, in fact after 210 minutes we observe three consecutive equal gap messurement. We then assumed that the specimen reached thermal equilibrium with a delay of 30 minutes.

Tempo	T	ΔL
min	°C	[μm]
180	30	16
195	30	17
210	30	18
225	30	18
240	30	18

Table 5.2: Investigation of thermal equilibrium in heating ramp.
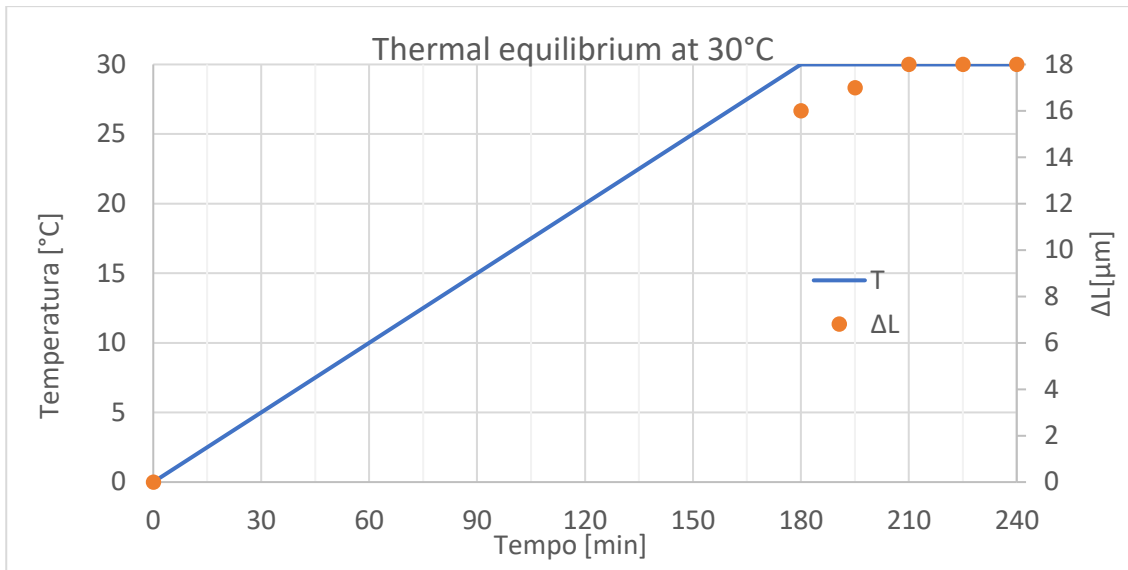
Figure 5.3: Investigation of thermal equilibrium in heating ramp.

5.1.1.2   **Core temperature variation**

Thermal equilibrium can be identified as the moment in which the temperature through all the cross section of the specimen is the same. By monitoring the core's temperature, we can obtain the time needed to have the same temperature in the measuring cell and in centre of the specimen. The following test performed to obtain the information needed

In Figure 5.4 it's shown the specimen and configuration used for the investigation. On the right part we can observe the asphalt concrete specimen the was drilled along its vertical axe from the top face up to a depth of 4 cm. A Type K Thermocouple connected with a digital datalogger (left side of Figure 5.4) was insert in the specimen and sealed with bitumen.

Figure 5.4: Asphalt concrete specimen equipped with type k thermocouple (right side) and datalogger (left side)

The method was carried out at the following temperature: 20 °C, 30 °C and 40 °C. The measuring cell's temperature was set to 20 °C, followed by a waiting period to guarantee the thermal equilibrium of the sample. A heating rate of 10 °C/h was used to change the temperature. Once the target temperature was reached the measuring cell was set at that constant temperature and the temperature of the core of the specimen was monitored until the same temperature as the measuring cell was reached.

In Table 5.3 and Figure 5.5 are reported the data registered during the test method performed. Comparing the slope of the temperature change measured in the measuring cell (blue line) and in the specimen's core (orange points) we can observe that the two slopes are different and as expected at first the specimen temperature is changing slower than the measuring cell due to thermal inertia. After a certain amount of time (about 30 min) the temperature in the measuring cell and in the specimen's core change at the same rate. The same delay is observed at the end of the change in temperature. This time is implemented in the method and used as the time needed by the specimen to reach thermal equilibrium after the measuring cell has reached the target temperature

Tempo	Measuring cell	Specimen
min	°C	°C
0	20	20
30	25	23.3
60	30	27.9
90	30	29.9
120	30	30
150	35	33.2
180	40	38.5
210	40	39.9
240	40	40
270	40	40
300	35	36.4
330	30	31.6
360	25	26.9
390	20	22
420	20	20.1
450	20	20

Table 5.3: Temperature profile of specimen and measuring cell
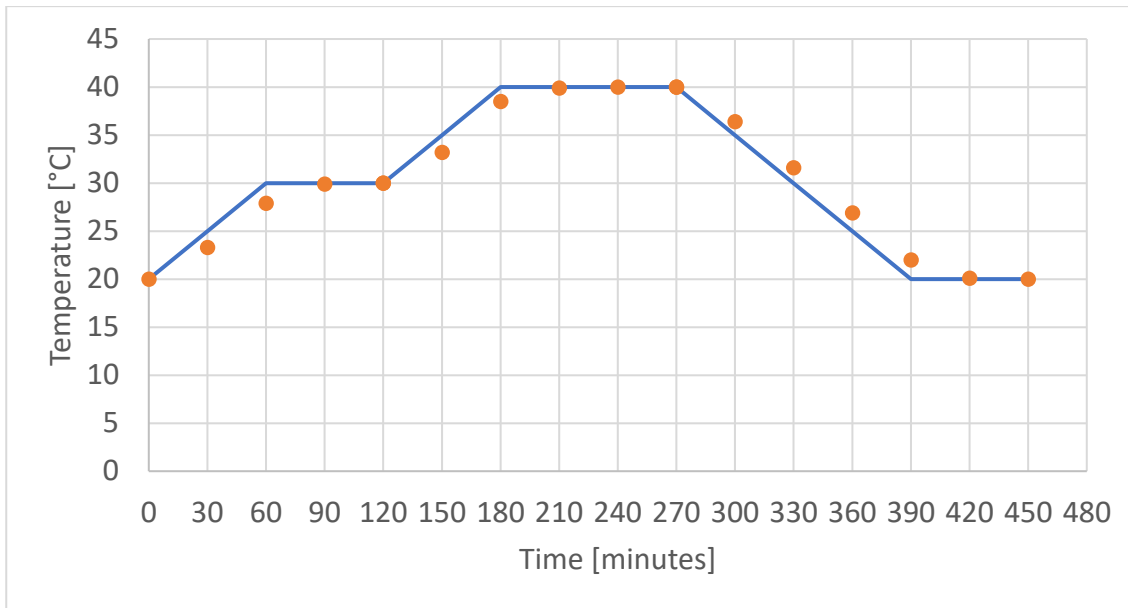
Figure 5.5:Temperature profile of specimen and measuring cell

5.1.2 Thermal deformation of the measuring system

In the test discussed in paragraph 5.1 the instrumental setup provide that the measuring system remains in the parking position during change of temperature. The measuring system is sufficiently distant from the hood. However, the air flow coming out could induce thermal deformations. Therefore, the air temperature near the plate was monitored placing a thermocouple, as shown in Figure 5.6, while the temperature in the measuring cell was at the two extreme temperatures of 40°C and -20°C.

In Table 5.4 are reported values of the air temperature around the upper plate at different time. In the second column are reported air temperature values observed when inside the temperature device we have 40 °C while in the third column are reported air temperature values observed when inside the temperature device, we have -20 °C. We can see that the air around the plate remains almost constant and the variation in temperature are probably linked with change in temperature of the laboratory. In any case with such variation in temperature thermal deformation are small enough to be neglected.

54

Figure 5.6: monitoring the air temperature near the measuring system with a thermocouple

Tempo	Measuring cell @ 40°C	Measuring cell @ -20°C
	T	T
min	°C	°C
30	24	23
60	23.5	22
75	25	22
90	24.7	22.2
105	25	23
120	26	23

Table 5.4:air temperature values around the measuring system

Since we assured that the measuring system does not deform in its parking position, we want to verify the also the temperature device, concentric cylinder C-PTD 200, does deform itself. Using a reference material with well known CTE it is possible to verify this condition. Indeed, if measuring its deformation in a specific temperature range the values will differ from those expected, we can assume that the C-PTD 200 is deforming under temperature changes. An Invar36 rod was used for this investigation since its CTE is very low and well known being equal $1.2 \times 10^{-6}\,°C^{-1}$.

Since the invar rod had small cross section a plastic support was crafted in order to support it during the test. In Figure 5.7 it's shown the crafted support and a top view of the sample inside the C-PTD 200.
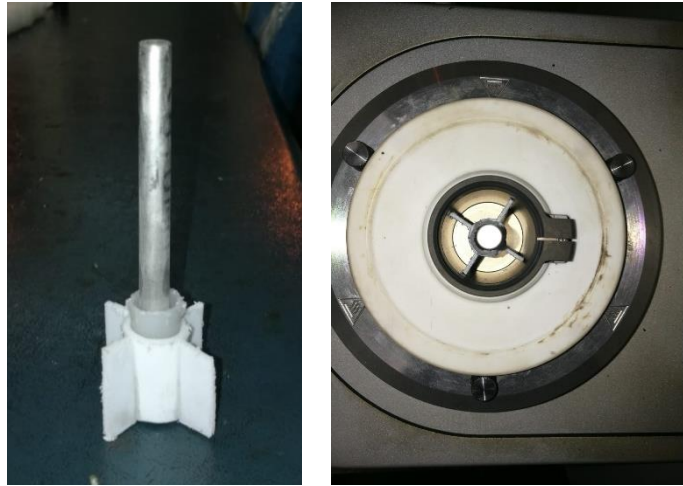
Figure 5.7: Invar Rod on its Plastic support (left) top view of C-PTD 200 with Invar sample inside.

The Invar rod was tested at the two temperatures 40 °C and 10°C. The temperature is kept constant and gap measurements are made every 15 minutes. When no gap variation occurs after 3 measurements in a row it's assumed that the specimen has reached the thermal equilibrium. Using the two-thermal equilibrium measurements we can compute the deformation and so the CTE. The CTE obtained by the investigation equals 1.17×10^{-6} °C^{-1}. This means that the instrumental setup does not contract, or deformations are so small that can be neglected.

By default, every measuring system and accessory has in its properties an Adjustment Gap Control (AGC). Measurements are adjusted applying this coefficient that takes into account thermal deformation of the measuring system.

For our tests AGC was set to zero since, as proven in the validation discussed before, with the instrumental configuration the measurement system is not affected by temperature.

In Figure 5.8 it's shown a screen shot of the dialog box where properties of the measuring system can be controlled. Enlighted with the red frame we can see that the AGC coefficient was set equal zero.
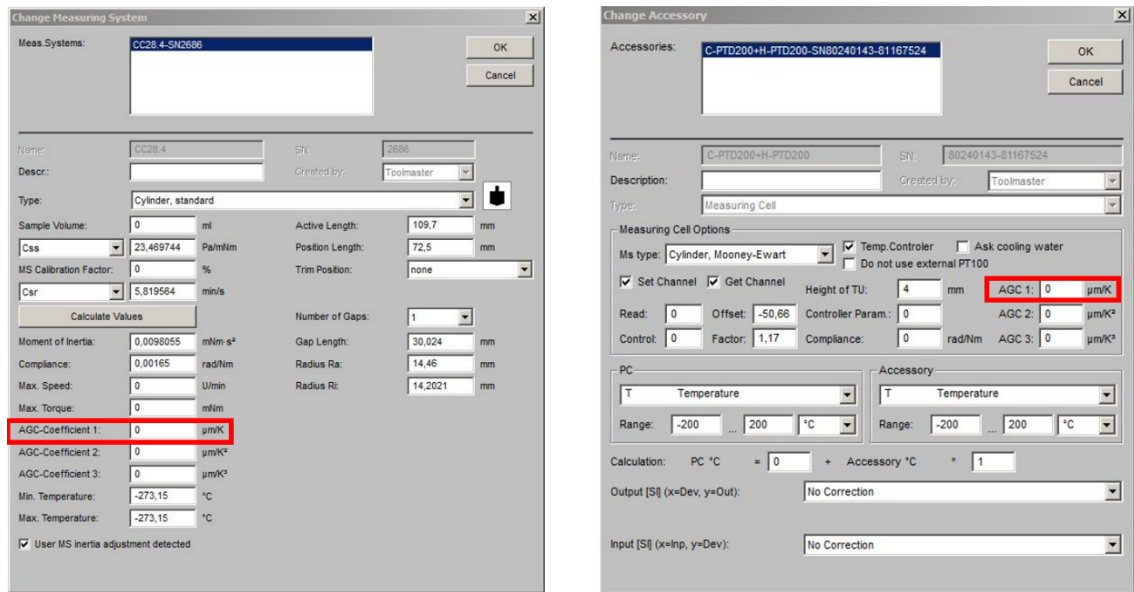
Figure 5.8: Dialog box for measuring system (left) and measuring cell properties (right)

5.2 Measurement with constant thermal ramp and contact

In paragraph 5.1 we discussed the test performed in thermal equilibrium. Between two consecutive measurement we don't have any information about specimen deformations. Furthermore, test required long time to be performed.

To have a detailed description of the phenomenon we decided to use a constant contact between the measuring system and the specimen. In this way we can perform measurement every 10 second. In order to have a shorter test time we used a thermal ramp with a speed of 10 °C/h without any resting time thaw oud ensure thermal equilibrium. A constant normal force of 0.1 N is applied. This amount of force is enough to ensure contact between specimen and measuring system and low enough to prevent mechanical deformation.

Performing the test without ensuring thermal equilibrium will induce some errors in the correct evaluation of CTC. In Figure 5.9 there's a qualitative representation of the temperature profile of specimen and measuring cell during time. We observe that as the thermal ramp starts the specimen temperature is not affected at first. Due to thermal conductivity the temperature change will take some time to reach core's temperature generating a delay in the temperature profile of the specimen. As temperature change reaches the specimen core's temperature starts changing at the same rate of the measuring cell.
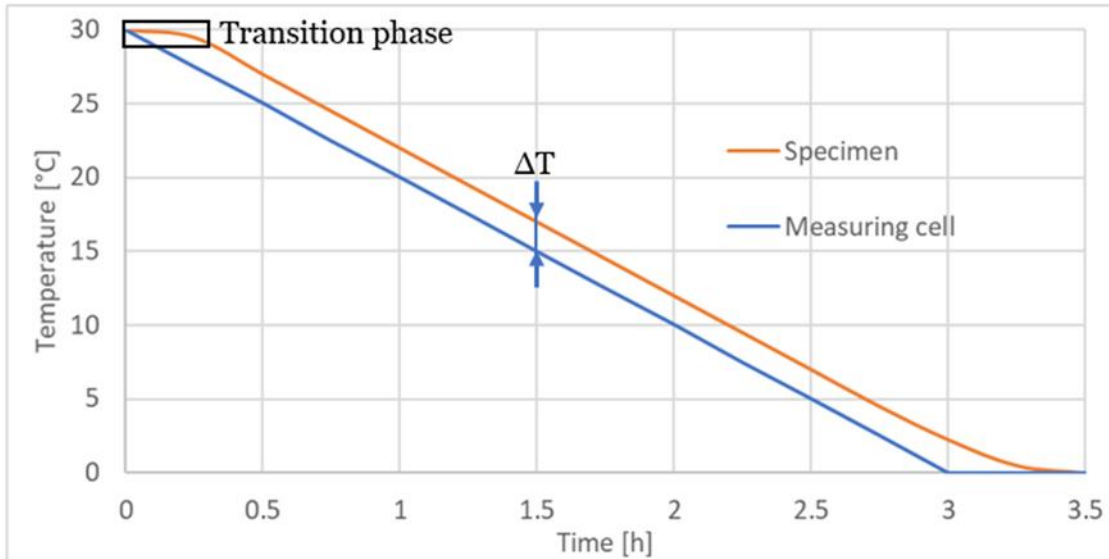
Figure 5.9: Qualitative representation of the temperature trend in the specimen and in the measuring cell.

This effect is important to consider when we want to evaluate an instantaneous CTE or CTC. In fact, considering the plot of strain versus temperature, the temperature we read it's referred to the measuring cell, but the corresponding specimen's strain we read must be referred to the specimen's core temperature that is higher than temperature of the measuring cell. Hence, we can't refer punctual values of strain to specific temperature, but since the decrease of the core's temperature has the same speed of the measuring cell, if we fit the strain trend with a linear regression his slope can be considered as the average CTC associated with our temperature range.

Figure 5.10 show the plot of strain versus temperature of a test conducted on an asphalt concrete specimen with a cooling ramp at the rate of 10 °C/h. It's possible to appreciate the initial delay discussed before (orange line). When analysing the data, the values registered during the delay will be neglected since they would influence CTC value.
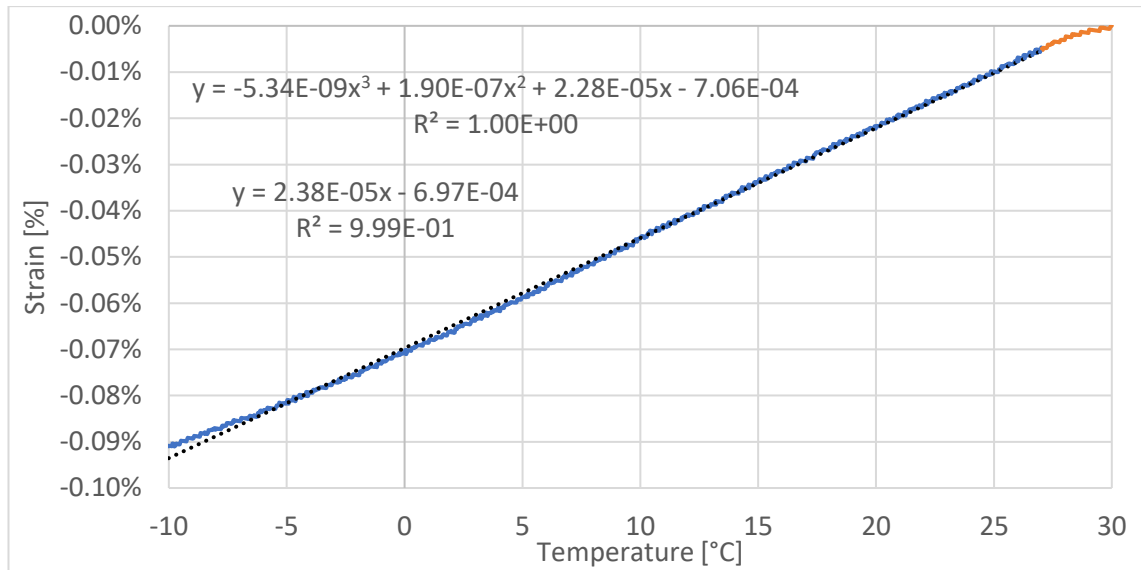
Figure 5.10: Representation of a test conducted on an asphalt concrete specimen

To better analyse the data obtained the trend was fitted with a linear and a polynomial regression the was the one giving best fit solution (Figure 5.10**Errore. L'origine riferimento non è stata trovata.**). This kind of trend was also found in Zeng and Shields [8] study where the trend had steeper slopes at higher temperatures and more horizontal at lower temperatures.

Considering the equation of the polynomial regression of strain versus temperature shown in Figure 5.10, it is possible to obtain the values of the instantaneous CTC by computing the slope at a specific point resulting in a variable CTC through all the temperature range (Figure 5.11**Errore. L'origine riferimento non è stata trovata.**).
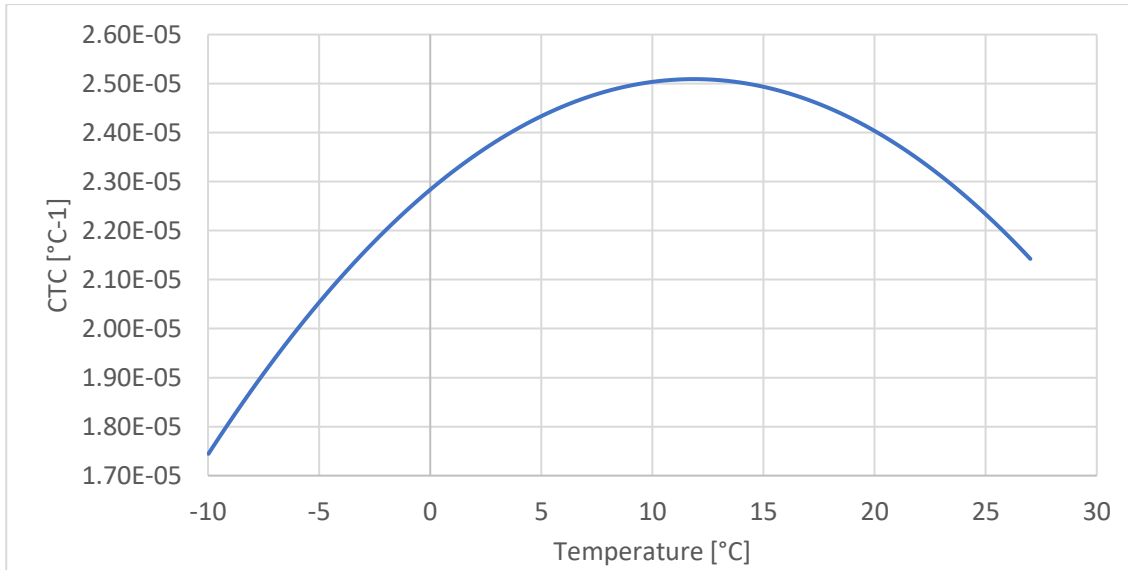
Figure 5.11: CTC of asphalt concrete specimen evaluated on the slope of a polynomial regression

To compare the results of the different method we prefer to refer to the mean value of CTC, and for this reason we will take into account the value of the linear regression shown in Figure 5.10 whose slope is the mean value of CTC in the temperature range investigated.

5.2.1 Measuring system's calibration

During the thermal ramp the measuring system will undergo temperature changes and inevitably it will deform. This must be considered when computing the CTE since the deformations we will obtain includes asphalt concrete deformations and measuring system deformations. It is necessary to know the thermal expansion and contraction of the measuring system in order to determine the actual deformation of the specimen. In the following paragraph will be explained the method used to calibrate the measuring system.

To determine the thermal deformation of measuring system the method developed is performed on an INVAR rod with well known and low CTC. INVAR is a is a nickel–iron alloy with 36% of nickel generically called FeNi36. Invar has a mean CTC value of $1.2 \cdot 10^{-6} \, °C^{-1}$ in the temperature range between 20 and 100°C was tested using the same method describe in the previous paragraph. In Figure 5.12 is represented the total deformation versus temperature. The final deformation we obtained is sum of the contraction of measuring system and of

the INVAR rod. Since we know the coefficient of thermal contraction of the INVAR, we can subtract it obtaining the contraction of the measuring system.
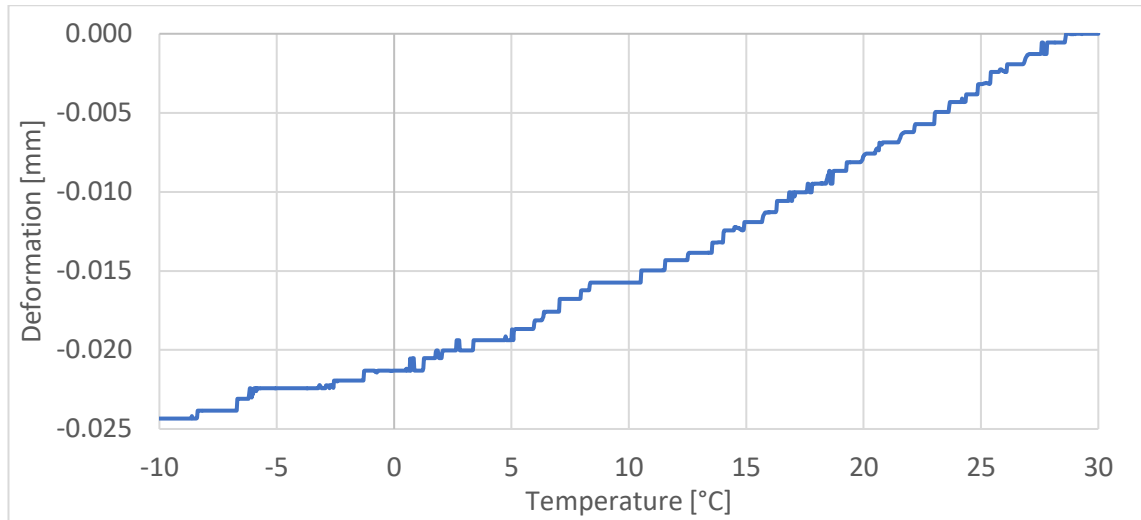
Figure 5.12: Investigation on instrumental deformation

Assuming the thermal deformation of the measuring system to be linear we can correct the measurement made on the asphalt concrete. We can observe in Figure 5.13 how not considering the measuring system's deformation could lead to significative difference in the evaluation of the CTC. The orange curve is the one that doesn't consider thermal deformation of the measuring system, the blue line is the what we obtain considering this deformation. In the first case we obtain a steeper slope than the uncorrected one.
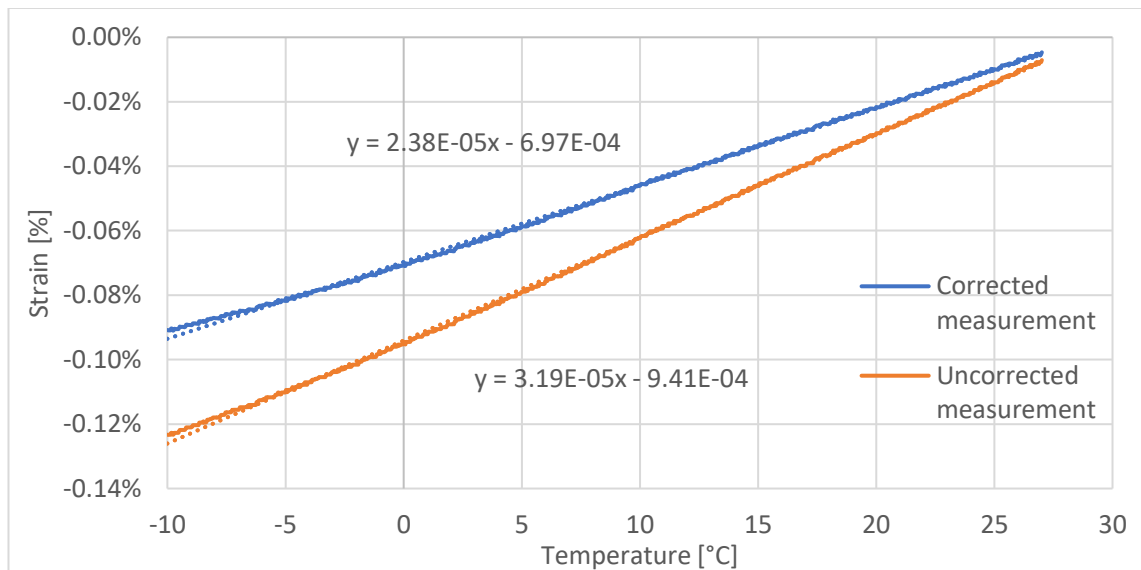
Figure 5.13: Comparison between corrected and uncorrected measurement

5.3 Measurement with Constant thermal ramp and no contact

Based on the previous tests a third method was developed in order to keep the benefits of them. To avoid any uncertainties due to thermal deformation of the measuring system we want to keep it as much as possible outside of the environmental chamber. A constant thermal ramp is used in order keep the duration of the test as short as possible.

Before the test start measurement of the specimen are made at room temperature to determine the L_o dimension with a caliper.

After 2 hours at the starting temperature to ensure that the specimen is in thermal equilibrium the first measurement is made. The thermal ramp starts with a speed of 10 °C/h and measurement are made with a step of 2 °C that corresponds to a time interval of 12 min. During the measurement the thermal ramp stops until the measurement it's complete and then it starts again at the same rate.

As for the test exposed in paragraph 5.2 the measurement made is not linked with the temperature we read since the specimen has higher temperature than the measuring cell, but for the same reason explained before the slope of a linear regression will give the mean value of CTC.
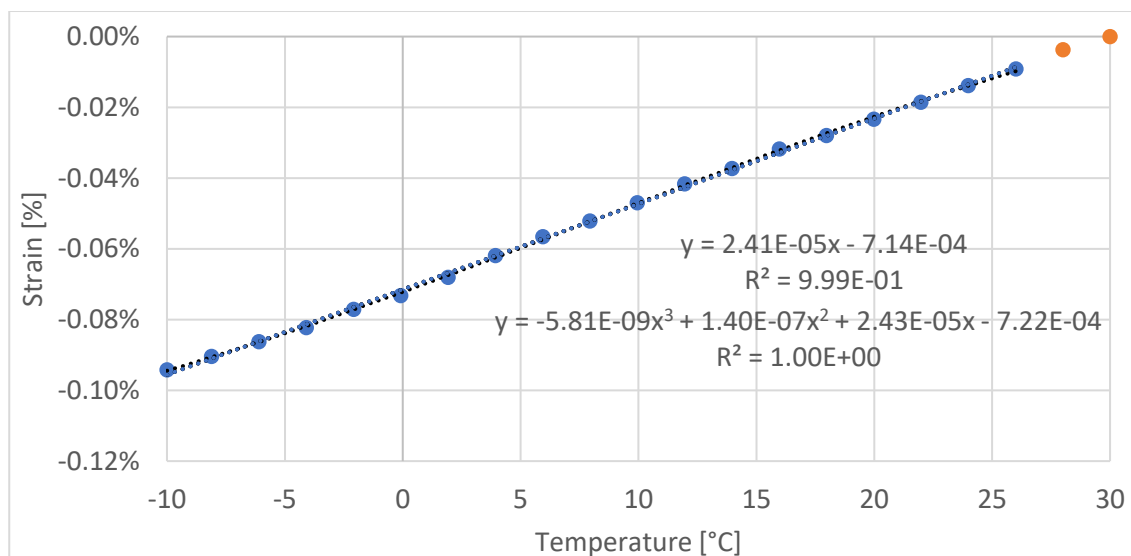
Figure 5.14: Height measurement of asphalt concrete specimen obtained with the third method

The equations shown in the figure:

$$y = 2.41E\text{-}05x - 7.14E\text{-}04$$
$$R^2 = 9.99E\text{-}01$$

$$y = -5.81E\text{-}09x^3 + 1.40E\text{-}07x^2 + 2.43E\text{-}05x - 7.22E\text{-}04$$
$$R^2 = 1.00E\text{+}00$$

In Figure 5.14 is represented the result of a test conducted on the same asphalt concrete used for the two other test. Even if it's not so evident also in this test due to thermal conductivity the temperature change will take some time to reach core's temperature generating a delay in the temperature profile of the specimen. As temperature change reaches the specimen core's also the deformation of the specimen starts. When analysing the data, the values of the first two measurement (orange bullets) will be neglected since they would influence CTC value.

Measured data were fitted with a linear regression and a polynomial regression of third degrees. In Figure 5.14 the two linear regression performed shows really small difference in R^2, more specifically the polynomial regression is the one that better fit the trend as in the previous test it's not significatively different.

In order to perform a comparison between the three method also in this case the linear regression (Figure 5.14) was chose and his slope is the mean CTC of the specimen tested. The CTC found is equal to $2.41 \cdot 10^{-5} \, °C^{-1}$ that is still comparable with those found in others studies as shown in Table 3.1. Furthermore the value found with this third method it's similar to the one found with the second test of paragraph 5.2 where the CTC is equal $2.38 \cdot 10^{-5} \, °C^{-1}$.

5.4 Method's comparison

An asphalt concrete specimen was tested in the temperature range from 30 °C to -10°C using the three different methods discussed in the paragraphs above.

In the first method the specimen's heights are measured only when thermal equilibrium is reached at four specific temperatures. Every temperature step is made applying a thermal ramp of 10 °C/h after which there's a resting time at the target temperature to ensure thermal equilibrium through all the specimen's depth. The measuring system enters the measuring cell only when the equilibrium is reached.

For the second method a thermal ramp is imposed through all the temperature range chosen with a speed of 10°C/h. This imply that specimen never

reaches thermal equilibrium and a difference between surface and core's temperature will be always observed causing uncertainties on the evaluation of CTC and CTE. Heights measurements are taken every ten second. For this reason, a constant contact between specimen and measuring system is required and it's ensured by applying a constant normal force of 0.1 N. Since the measuring system undergo temperature's changes it's deformation must be take into account when evaluating CTC and CTE.

The third method is thought as combination of the two methods exposed before. The measuring system is kept outside the measuring cell and heights measurement are taken with step of 2 °C without ensuring thermal equilibrium. The thermal ramp is imposed through all the temperature range chosen with a speed of 10°C/h

Specimen's dimensions were measured with a caliper at the room temperature. Before each test started the specimen was first kept at the starting temperature of 30 °C to ensure thermal equilibrium and at this specific temperature the strain is considered equal zero. At the end of each test the data obtained are plotted in terms of strain versus temperature where strain is computed as:

$$\varepsilon = \frac{\Delta L}{L_0} \cdot 100$$

Where:

- ΔL is the deformation of the specimen between two consecutive measurements;

- L_0 is the length of the specimen performed at room temperature.

For each method CTC values were determined as the slope of the linear regression performed through all the temperature range. Since the second and the third test are not conducted in thermal equilibrium, the linear regression was performed on the data neglecting the measurements made during the delay time. Due to thermal conductivity the temperature change will take some time to reach core's temperature generating a delay in the temperature profile of the specimen and considering this transition phase in the regression could induce error in CTC determination.

64
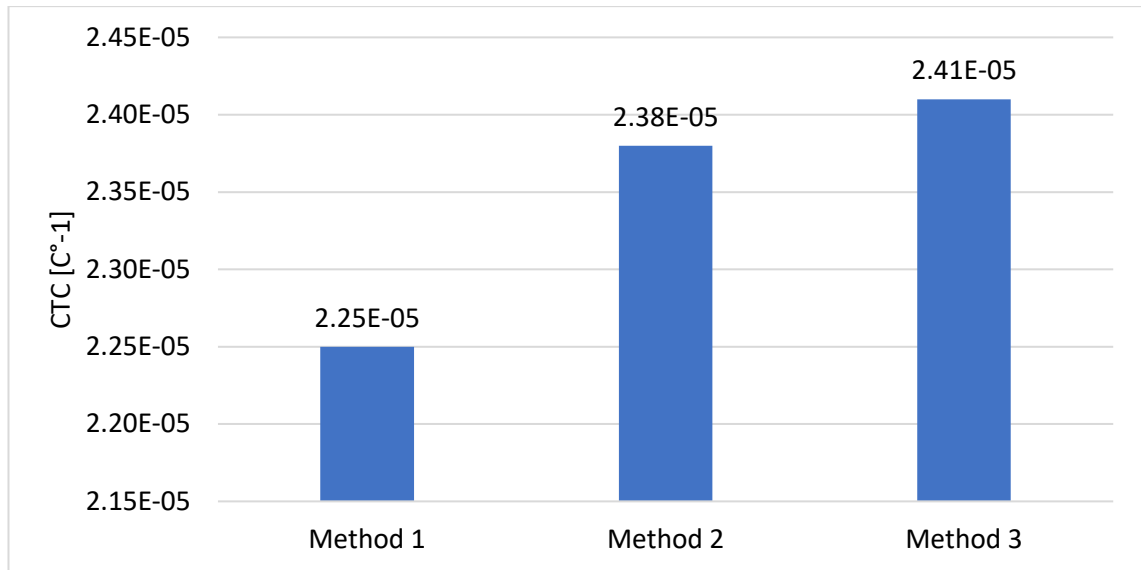
Figure 5.15: CTC obtain on a sample of AC using the three tests method

In Figure 5.15 are reported the mean value of CTC obtained with the three methods. While method 2 and 3 give similar values, they differ significatively from the first procedure. More specifically method 2 and 3 have higher CTC than method 1. Method 2 and 3 are not conducted in thermal equilibrium and so the greater contraction expected was in the method 1 since it is the only method where the specimen has the time to fully transform thermal stresses in deformation.

In Figure 5.16 the trend obtained with the three methods are compared. The three trends overlay almost perfectly in the range temperature between 10 and 14 °C while they diverge at low and high temperature. This discrepancy is probably linked to thermal deformation of the measuring system. In fact, while in method 1 the measuring system is outside the system in method 2 is constantly inside the measuring cell while in method 3 it underwent several times to temperature differences.
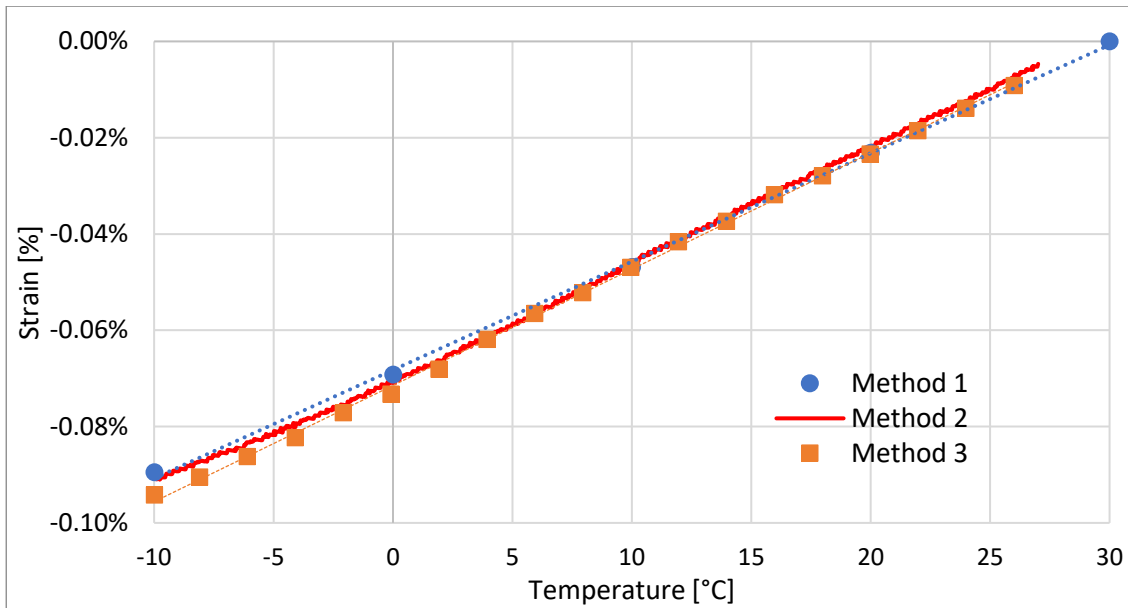
Figure 5.16: Comparison of measurements and trends obtained with the three tests method

The first method is the one giving the

5.5 Method's Validation

To validate how well the instrumental setup and the methods developed can capture the correct value of CTC and CTE, different materials were tested using a similar method to the one explained in the first paragraph. To fully comprehend the goodness of the methods the material where chosen so that we could have a great variety of CTC.

Not all the materials were easy to be shaped and for this reason their dimensions are different but all of them have a cylindrical shape.

The INVAR rod used for the test in Figure 5.17 has a length of 100 mm and cross section of 8 mm. The ceramic specimen was realised by a local artisan and differently from the other specimens it is a hollow cylinder with a height of 80 mm and diameter of 30 mm. The aluminium specimen has a cross section with a diameter of 20 mm and a height of 80 mm. Stainless steel specimen is 80 mm long with a diameter of 25 mm.

66

Figure 5.17: From left to right, Invar, ceramic, stainless steel and aluminium samples

The method performed to test these specimens is similar to method 1. We want to evaluate the CTC in thermal equilibrium but because their variety of dimensions the time needed to reach thermal equilibrium is different for each one of them. To be sure that every specimen is in thermal equilibrium the following method was developed.

The specimen is measured with a caliper at the room temperature and length registered is considered the L_0. Three specific temperature 40, 15 and - 10 °C are investigated. The specimen is kept at the starting temperature of 40 °C for 1 hour after which heights measurement are performed every 15 minutes and when three consecutive equal readings occur it is assumed that the thermal equilibrium is reached. A temperature rate of 20 °C/h is used to reach the next target temperature and procedure continue as for the first step.

At the end of the test the heights measured at thermal equilibrium are plotted in terms of strain versus temperature where strain is computed as:

$$\varepsilon = \frac{\Delta L}{L_0} \cdot 100$$

Where:

- ΔL is the deformation of the specimen between two consecutive measurements;

- L_0 is the length of the specimen performed at room temperature.

For each material the mean CTC value is determined as the slope of the linear regression obtaining the mean CTC in the temperature range from 40 to - 10 °C.

In Figure 5.18 are summarized the mean CTC values measured compared with those found in literature. The method developed shows to be capable to evaluate with great accuracy the CTC values.

	Invar	Ceramic	Aluminium	Stainless steel
■ Literature	1.2E-06	7.5E-06	23.0E-06	17.0E-06
■ Measured	1.2E-06	7.5E-06	23.0E-06	17.0E-06
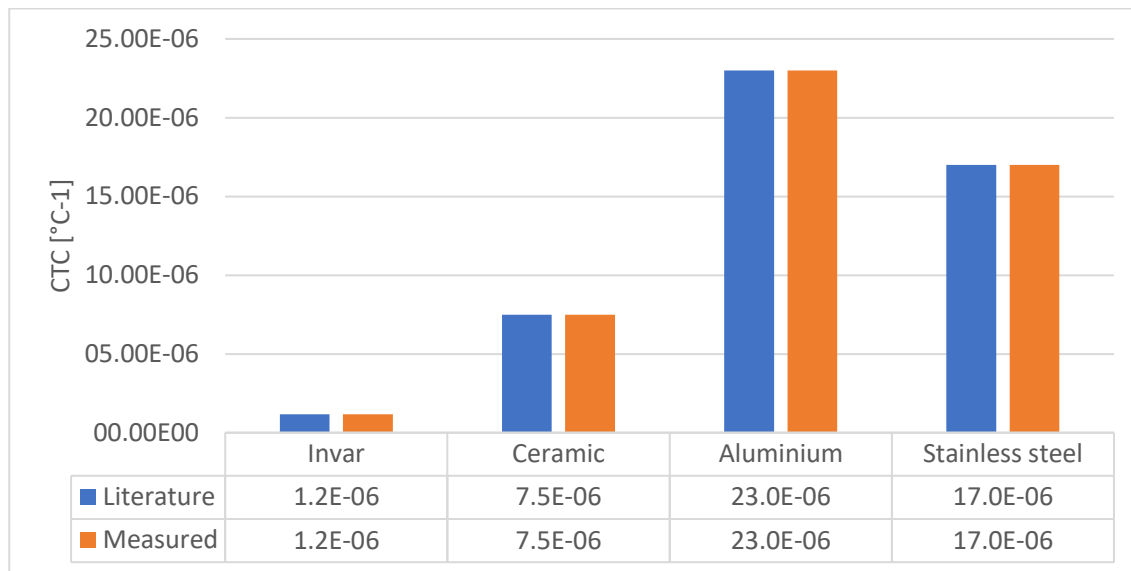
Figure 5.18:CTC values for different materials

It is possible to observe that the first method proposed is able to evaluate with great precision the CTC of different material.

5.6 Thermal Cycle

To investigate the repeatability of the method different thermal cycle were applied to a sample of Aluminium obtaining the same value for each cycle. Same procedure was then applied to and asphalt concrete cylinder. In this case was observed that not only CTC and CTE are different but their values also depend from their thermal history. Indeed, was observed that cycle by cycle the CTC values decrease while CTE shows the tendency to increase. Since the test method was first validated with a known material, we can exclude that this behaviour it's caused by the instrumental setup and affirm instead that is linked with to the viscoelastic properties of the material.

68

When a solid elastic material undergoes a thermal cycle of heating and cooling shows no differences in terms of CTC and CTE and follow the same deformation path (Figure 5.19-a). On the contrary Asphalt concrete shows differences between CTC and CTE, more specifically was observed that CTC has higher values than CTE [8]–[10]. In terms of deformation this means that after a cycle of cooling and heating asphalt concrete shows permanent length changes (Figure 5.19-b).

(a)   (b)
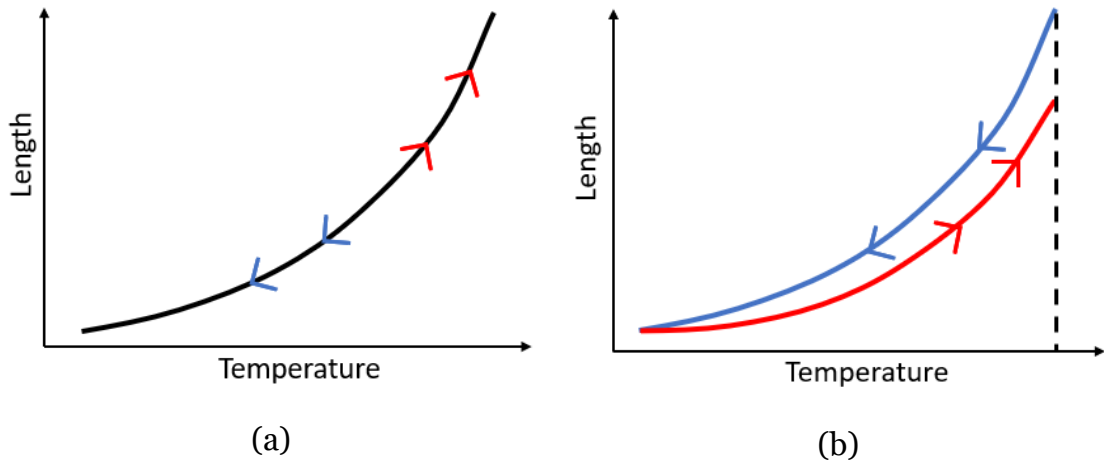
Figure 5.19: deformation path for solid (a) and asphalt concrete (b)

One hypothesis is the densification of AC due to irreversible expansion and contraction of the bitumen in the air voids [8]. Gravity can be another factor that cause the difference between the two parameters creating resistance during the expansion of the specimen.

The methods used is the same as the one used to validate the method. The specimen is kept at the starting temperature for 2 hours to ensure its thermal equilibrium. The method consists in measuring height of the specimen at three specific temperature 40, 15 and -10 °C during a cooling and a heating ramp. Transition from two target temperature is made using a rate of 20 °C/h. Once temperature target has been reached, measurements are performed every 15 minutes and when three consecutive equal readings occur it is assumed that the thermal equilibrium is reached. The difference between the two heights measured at the thermal equilibrium are the thermal deformation used to compute CTC if the we are considering the cooling path or CTE if we consider the heating ramp.

At the end of the test the heights measured at thermal equilibrium are plotted in terms of strain versus temperature where strain is computed as:

$$\varepsilon = \frac{\Delta L}{L_0} \cdot 100$$

Where:

- ΔL is the deformation of the specimen between two consecutive measurements;

- L_0 is the length of the specimen performed at room temperature.

5.6.1 Thermal Cycle on aluminium

To investigate the repeatability of the method different thermal cycle were applied to a sample of Aluminium.

In Figure 5.20 are reported heights measurements performed at all the target temperature investigated in the test which are 40, 15, -10 °C. As expected, no permanent deformations are observed. At the end of each cycle the aluminium specimen once reached the thermal equilibrium at the starting temperature always shows the same length.
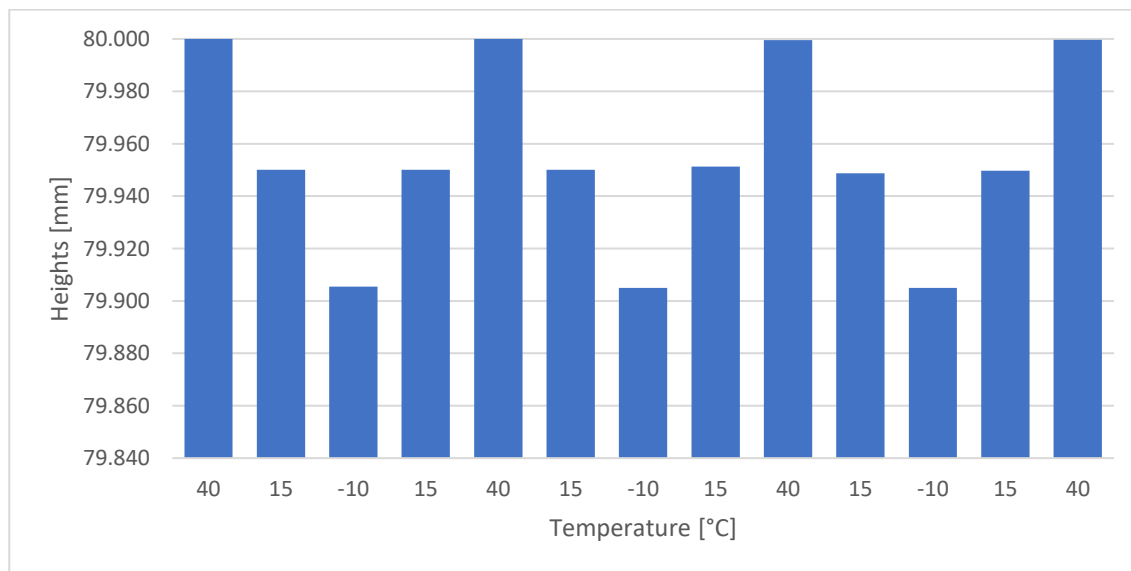

Figure 5.20: Aluminium specimen's heights and deformations at each target temperature of the thermal cycles

The test method is performed at three specific temperature 40, 15 and - 10 °C in cooling and heating condition. It is then possible to evaluate CTC and

70

CTE between two consecutive temperature steps as the slope of their linear regression. So in this specific test for each cycle we can evaluate two different CTC for the cooling ramp, one from 40 to 15 °C and one from 15 and -10 °C, and two different CTE for the cooling ramp, one from -10 to 15 °C and one from 15 and 40 °C.

Figure 5.21 summarize the values obtained and commenting them we will refer to the range between 40 and 15 °C as high temperature and the range between 15 and -10 °C will be called as low temperature. It is possible to appreciate that CTC and CTE varies from low to high temperature. In fact, for all solid material their coefficient is considered linear for practical reason, but their real trend is not a linear function and CTE can vary considering different temperature range.

It is possible to observe how the values highlighted with the red frame are the one that shows biggest differences compared with the others. It must be pointed out that the test took 36 hours to be completed and those specific measurement were conducted during the night. During the night the air conditioning system is switched off leading to different room temperature between night and day that could have possibly induced thermal deformation in the measuring system.

CTC [°C-1]	Cycle 1	Cycle 2	Cycle 3
■ 40 to 15	2.50E-05	2.50E-05	2.54E-05
■ 15 to -10	2.23E-05	2.25E-05	2.19E-05
■ -10 to 15	2.23E-05	2.31E-05	2.23E-05
■ 15 to 40	2.50E-05	2.41E-05	2.50E-05
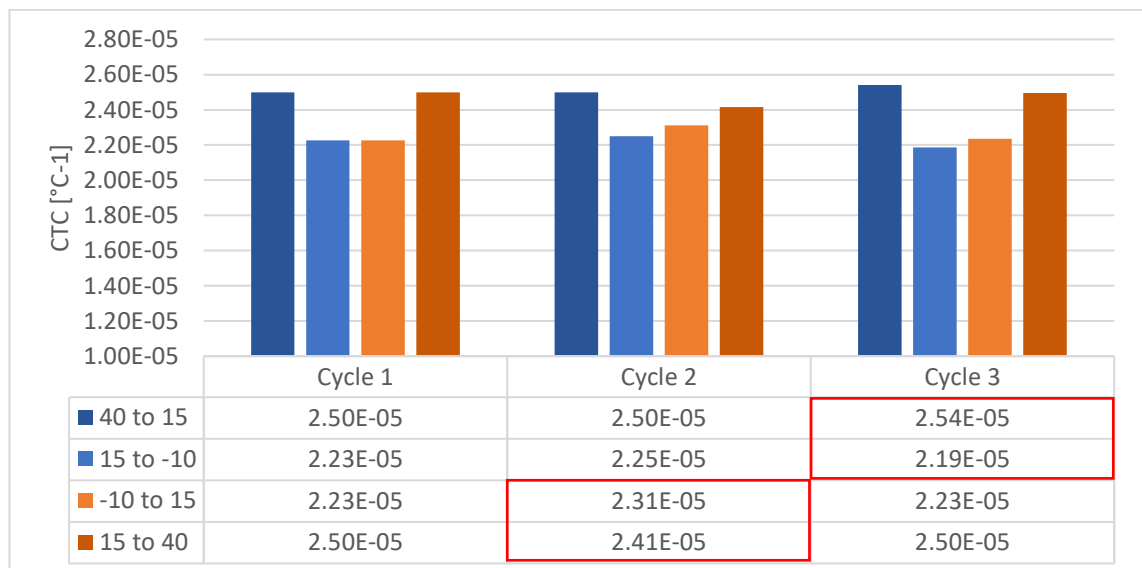
Figure 5.21: Aluminium CTC and CTE values obtained in different thermal cycle for each temperature steps

Considering the strain versus temperature plot let's consider CTC and CTE evaluated as the slope of a linear regression on the three target temperature obtaining the mean CTC and CTE in the temperature range from 40 to -10 °C. Figure 5.22 summarize the results obtained. The tested material shows the same values of CTC and CTE during cooling and a heating ramp and through all the thermal cycles performed.

	Cycle 1	Cycle 2	Cycle 3
CTC	2.36E-05	2.37E-05	2.36E-05
CTE	2.36E-05	2.36E-05	2.36E-05
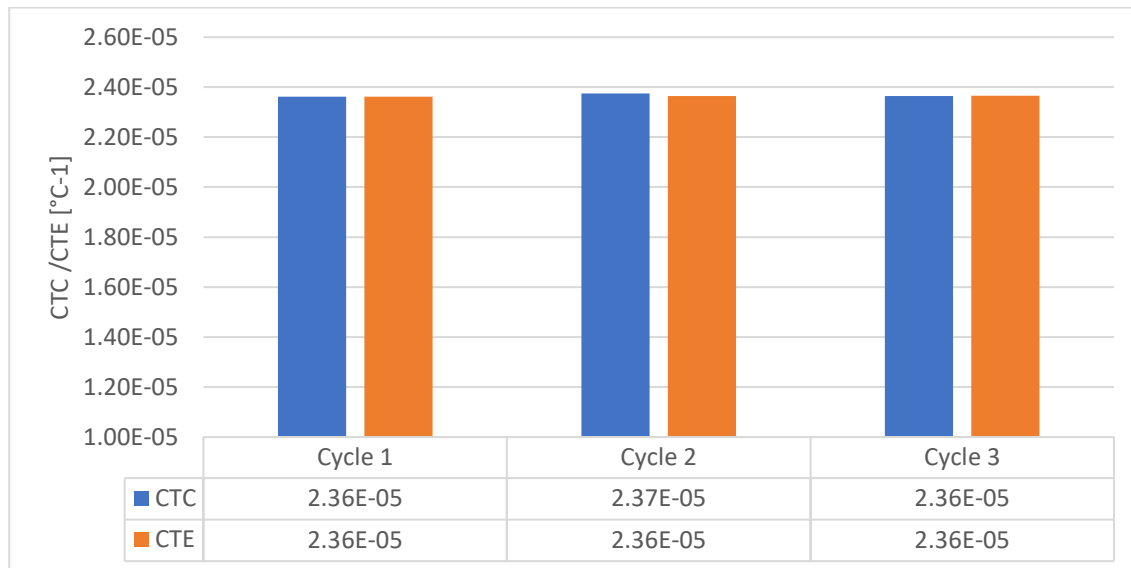
Figure 5.22: Aluminium CTC and CTE values obtained in different thermal cycle

5.6.2 Thermal Cycle on asphalt concrete

Same test performed for the aluminium is conducted on the asphalt concrete. Figure 5.25**Errore. L'origine riferimento non è stata trovata.** shows the heights of the asphalt concrete specimen measured at each target temperature after thermal equilibrium was reached. Cycle by cycle the specimen shows a permanent deformation in his length. We can observe at the end of the first cycle we have the biggest permanent deformation of 0.005 mm, at the end of the three cycle the total amount of permanent deformation equals 0.010 mm.

72
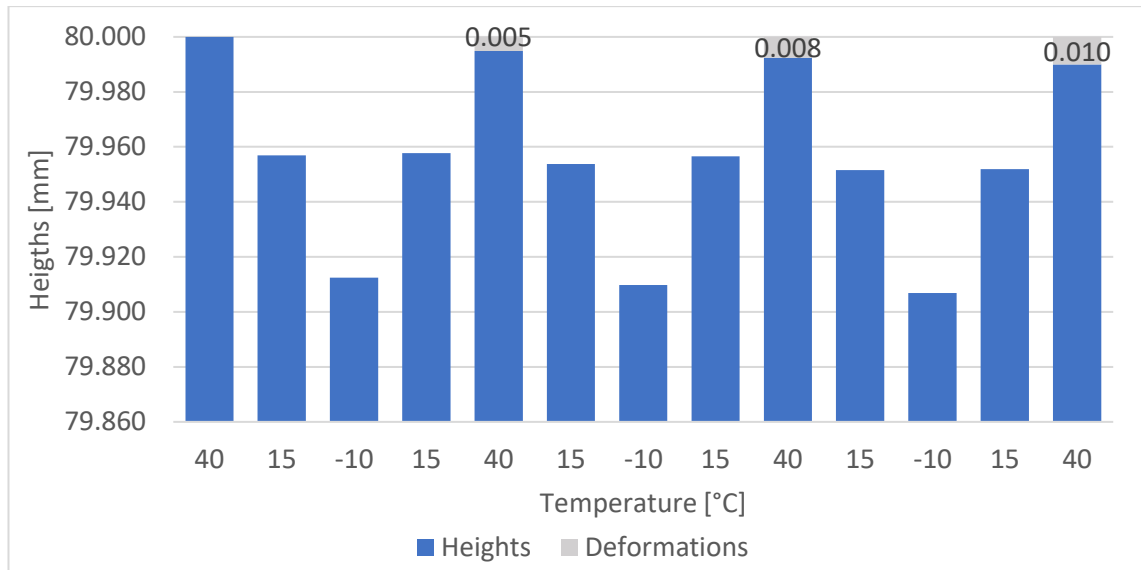
Figure 5.23: Asphalt concrete specimen's heights and deformations at each target temperature of the thermal cycles

The test method consists in measuring height of the specimen in thermal equilibrium at three specific temperature 40, 15 and -10 °C in cooling and heating condition. It is then possible to evaluate CTC and CTE not only through all the temperature range but also between two consecutive temperature steps as the slope of the linear regression between two measurements. So in this specific test for each cycle we can evaluate two different CTC for the cooling ramp, one from 40 to 15 °C and one from 15 and -10 °C, and two different CTE for the cooling ramp, one from -10 to 15 °C and one from 15 and 40 °C. The values obtained are summarized in Figure 5.24.

In the following analysis we will refer to the range between 40 and 15 °C as high temperature and the range between 15 and -10 °C will be called as low temperature. Since all cycles shows the same trend, we will focus the analysis on the single cycle. We can observe that at low temperature CTC and CTE show bigger values compared to higher temperature. While CTE at lower temperature shows higher values than CTC at high temperature we observe the opposite behaviour. Values of CTC and CTE between high to low temperature have the tendency to increase. More specifically the increase observed in CTE is more relevant than the one observed for CTC.

When cooled or heated asphalt concrete shows differences between CTC and CTE, more specifically was observed that CTC has higher values than CTE

73

[8]–[10] as also highlighted from our test method whose values are summarized in Figure 5.24. In terms of deformation this means that after a thermal cycle asphalt concrete shows permanent length change.

	Cycle 1	Cycle 2	Cycle 3
■ 40 to 15	2.16E-05	2.05E-05	2.05E-05
■ 15 to -10	2.22E-05	2.20E-05	2.24E-05
■ -10 to 15	2.26E-05	2.34E-05	2.25E-05
■ 15 to 40	1.85E-05	1.79E-05	1.91E-05
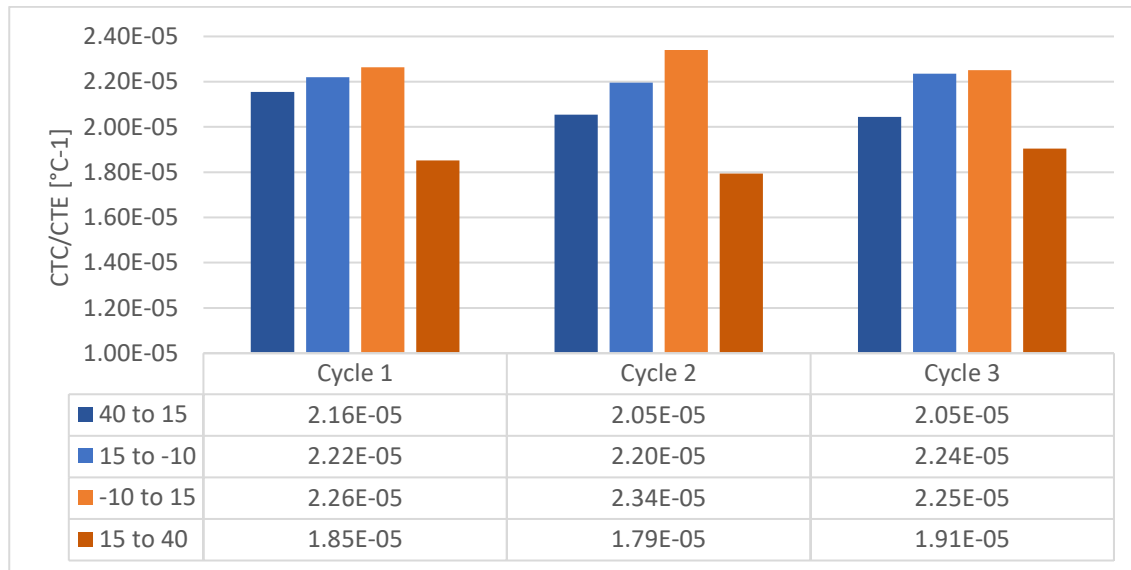
Figure 5.24: Asphalt concrete CTC and CTE values obtained in different thermal cycle for each temperature steps

Considering the strain versus temperature plot let's consider CTC and CTE evaluated as the slope of a linear regression on the three target temperature obtaining the mean CTC and CTE in the temperature range from 40 to -10 °C.

In Figure 5.25 are summarized the results of the test where for each cycle are represented CTC and CTE values. We can observe that not only CTC and CTE are different but their values also depend from their thermal history. Indeed, was observed that cycle by cycle the CTC value decreases while CTE shows the tendency to increase.

74

	Cycle 1	Cycle 2	Cycle 3
■ CTC	2.19E-05	2.13E-05	2.14E-05
■ CTE	2.06E-05	2.07E-05	2.08E-05
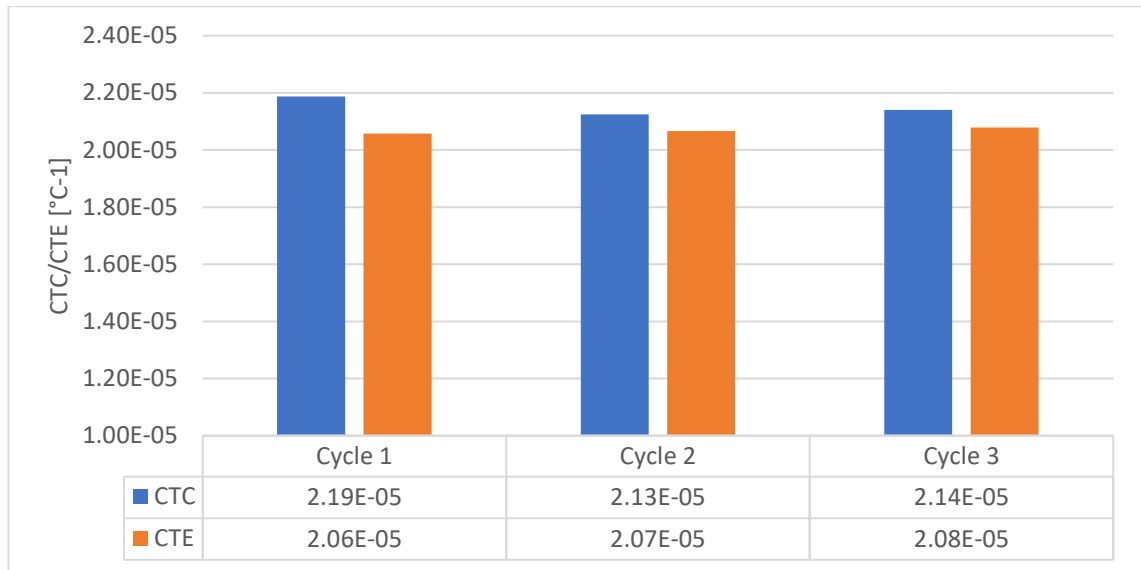
Figure 5.25: Asphalt concrete CTC and CTE values obtained in different thermal cycle

The values found are comparable with those found in literature in which was observed that CTC values vary between 2.1×10^{-5} and 3.33×10^{-5} °C^{-1} and CTE values instead vary between 1.85×10^{-5} °C^{-1} and 3.12×10^{-5} °C^{-1}. In general, was observed that CTC has higher values than CTE that is also possible to appreciate in the results obtained.

CTC values show higher variability than CTE. The biggest difference obtained in CTC is equal 0.06×10^{-5} while CTE values are more stable as the biggest difference is equal 0.02×10^{-5}.

CHAPTER 6

EFFECTS OF MIX CHARACTERISTICS ON CTE/CTC

In this chapter will be exposed a practical application of the first method. An asphalt concrete with known mix characteristic was compacted with four different compaction effort in order to obtain four different specimens with different voids percentage. The compaction effort levels chose are 180, 100, 50, 30. To evaluate if the air voids percentage affect the CTC and CTE the four specimen specimens obtained will be tested using the first method to evaluate their CTC.

The specimen is measured with a caliper at the room temperature and length registered is considered the L_0. Three specific temperature 40, 15 and - 10 °C are investigated. The specimen is kept at the starting temperature of 40 °C for 1 hour after which heights measurement are performed every 15 minutes and when three consecutive equal readings occur it is assumed that the thermal equilibrium is reached. A temperature rate of 20 °C/h is used to reach the next target temperature and procedure continue as for the first step.

At the end of the test the heights measured at thermal equilibrium are plotted in terms of strain versus temperature where strain is computed as:

$$\varepsilon = \frac{\Delta L}{L_0} \cdot 100$$

Where:

- ΔL is the deformation of the specimen between two consecutive measurements;

- L_0 is the length of the specimen performed at room temperature.

For each material the mean CTC and CTE values are determined as the slope of the linear regression obtaining the mean CTC and CTE in the temperature range from 40 to - 10 °C.

6.1 Material characteristic

Four specimens with different compaction effort are prepared to be tested and to evaluate the influence of air voids on CTE and CTC. The bituminous mixture used for the compaction of the four specimens was fully characterized in a previous study.

6.1.1 Binder content

This method consists in the separation of the bitumen and all the others volatile substances from the aggregates by means of an Asphalt Binder Analyzer. The Asphalt Binder Analyzer, also known as Carbolite, is a high precision apparatus combining an ignition oven with a continuous weighing system that monitors the loss of weight of the asphalt sample. When there are no more losses in weight the test ends and the Carbolite automatically determines the binder content and percentage.

In Table 3.1 are summarize the result of the test on four different sample and the average values obtained.

Sample	%Bmixture	%Baggregates
(-)	(%)	(%)
1	5.31	5.60
2	5.26	5.55
3	5.33	5.63
4	5.33	5.63
AVERAGE	5.31	5.60

Table 6.1: Binder contents values obtained with Asphalt binder Analyzer

6.1.2 Particle size distribution

The aggregates gradation is determined by means of sieving and weighting; it is performed with a sieve shaker that is activated by electromagnetic impulses and has a triple vibrating action (vertical, lateral and rotational); the vibration continues for 15 minutes.

Firstly, aggregates are washed using a sieve with an opening of 0.063mm, to remove the filler. The filler during the sieving can remain attached to the aggregates' surface, overestimating the measure of the weight of the retained material. After the washing the weight of loss will be considered as the content of filler in the material. Before the test the material is dried placing it in an oven at a temperature of 105 °C.

The material retained at each sieve is weighted and from the values obtain the curve of the progressive passing is built.

Different sample of the material were tested and in Figure 6.1 is represented the average curve of the particle size distribution.
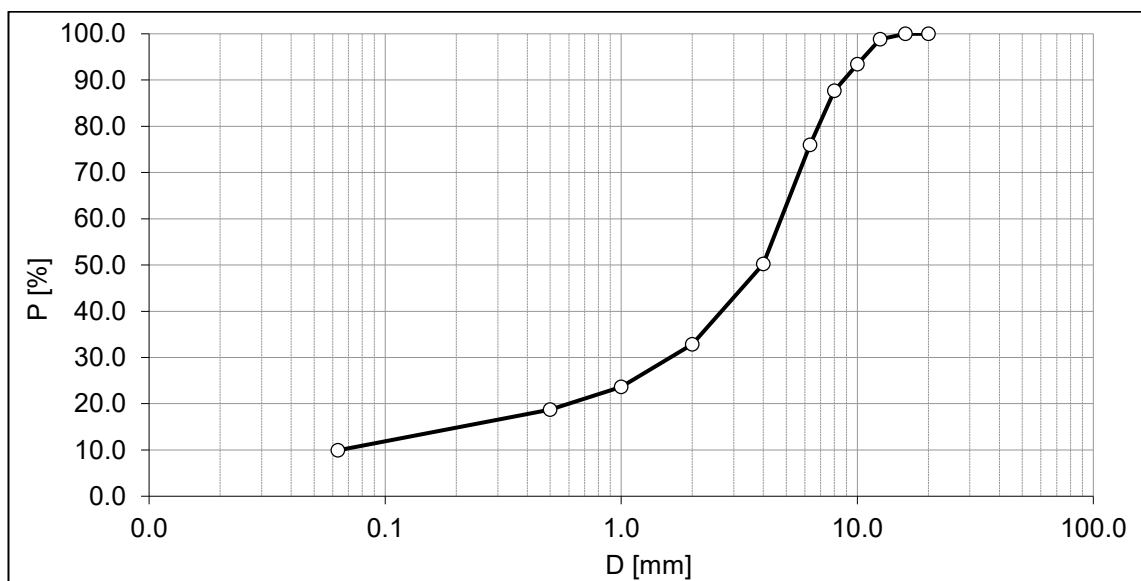

Figure 6.1: Particle size distribution

6.1.3 Theoretical Maximum density

The Theoretical Maximum Density (TMD) is the density of the mixture excluding air voids and it is determined using a sample of loose material and

calculating the volume of water it displaces, according to the (UNI EN 12697-5, 2003).

The mass of a pycnometer with its top cover are previously measured. A sample of loose material is placed inside a pycnometer and covered with its top and the total mass is recorded. Distilled water is poured in the pycnometer until the loose sample is fully covered and then by applying a vacuum the air inside the material's voids is removed. When the air is totally extracted, the vacuum is slowly released, and the pycnometer is covered with is top and filled with deaerated water. The mass of the filled pycnometer is registered as the temperature of the water to compute its exact volume.

The equation used to compute TMD is the following:

$$TMD = \frac{M_{p+m} - M_p}{1000 \cdot V_p - (M_{p+m+w} - m_2)/\rho_w}$$

Where:

- TMD is density of the sample [kg/m³];

- M_p: mass of the pycnometer and the top [g];

- M_{p+m} : mass of the pycnometer and the top, filled with the sample [g];

- $M_{p+m} + w$: mass of the pycnometer and the top, filled with the sample and water [g];

- V_P: volume of the pycnometer and the top [m³];

- • ρw: density of the water at test temperature [kg/m³].

Picnometer	M_P	M_P+M	M_P+M+w	V_P	T	ρw	ρmw
-	(g)	(g)	(g)	(m³)	(°C)	(kg/m³)	(kg/m³)
T+I	861.3	1374.9	2566.9	0.0013971	21.8	997.9	2536
7+B	893.8	1420.8	2572.2	0.0013617	22.0	997.8	2536
6+B	1016.0	1574.0	2639.3	0.0012877	23.0	997.6	2538
8+A	994.8	1600.5	2678.0	0.0013185	20.3	998.2	2534
6+I	1014.5	1557.8	2637.8	0.00129589	20.4	998.2	2540
						AVERAGE	2537

Table 6.2: Theoretical maximum density of mixture

6.2 Specimen's realization

To obtain the desired level of compaction the Gyratory Shear Compactor (GSC) is used, since it better simulates the action of the steamrollers during the construction phase; moreover, it allows to evaluate the density during the test. The machine can work setting number of gyrations as target or the final height of the specimen.

The bituminous mixture and a mould with an inner diameter of 150 mm are heated and when a temperature of 150 °C is reached the bituminous mixture is place in the mould. As the one shown in Figure 6.2.

Figure 6.2: mould used for the gyratory shear compactor

The machine, in Figure 6.3-a, is composed from a rigid body, a load element and a system that is able to measure heights of the specimen during the gyrations. During compaction a static compression of 600 kPa, and a shear force are applied on the specimen. As represented in Figure 6.3-b, the mould has an inclination angle of 1.25° in order to generate a conical revolution surface; this rotation creates in the specimen some shear forces that, combined with the static force, allows to reach the optimal densification, with a continuous rearrangement of the particles.
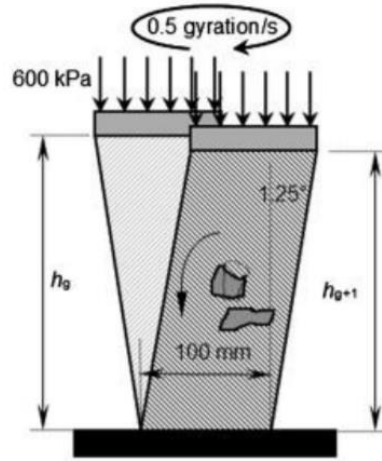
(a)   (b)

Figure 6.3: GSC Machine (left) and compaction mechanism (right)

Once the specimen where compacted they were cored in vertical position as shown in Figure 6.4 in order to obtain a homogeneous distribution of the voids inside the specimen. After the coring the specimen were cut with a saw machine of the desired dimension. In Figure 6.4-right are shown the four specimens obtained and tested.

Figure 6.4: Compacted sample (left), 80 mm sample cored and sawed (right)

6.2.1 Bulk specific gravity

The bulk specific gravity test evaluates the mass (comprehensive of air voids) per unit volume of the sample by the ratio of its weight and the weight of an equal volume of water. To obtain the value the sample weight is measured in three different condition.

The specimen is preventively dry in a climatic cell so to extract all the water inside and its weight measured in air is registered. The specimen is then is soaked

in water for an hour to give water the time to fill all the air voids inside the specimen. After an hour the specimen's weight in water is registered as the temperature of the water that will be used to compute its specific gravity. The sample is took out from the water and after the water on its surface is dried the sample is weighted again.

Bulk specific gravity is computed by mean of the following equation:

$$MV = \frac{M_D}{M_{SSD} - M_w} \cdot \gamma_{w,T}$$

Where:

- MV: Bulk specific gravity of the specimen;
- M_D: mass of the dry specimen in air [g];
- M_w: saturated mass of the specimen in water [g];
- M_{SSD}: saturated mass with dry surface in air [g];
- $\gamma_{w,T}$: Water specific gravity at the temperature T [kg/m³]

6.2.2 Voids content

Purpose of the valuation of the TMD that was obtained in a previous study and the MV value performed in this study is to determine the percentage of air voids present in the four specimens realized. The percentage of air voids contained within the sample is given by the following equation:

$$v \, [\%] = 100 \cdot \left(1 - \frac{MV}{TMD}\right)$$

In Table 6.3 are reported the voids values obtained for the four specimens. As expected, voids decrease as gyrations increase. Between 180 and 100 gyrations we observe very small variation. We observe that voids increase most between 100 and 50 gyrations .

Sample	M_{air}	M_{H2O}	M_{SSD}	T	ρ_w	MV	TMD	v
[-]	[g]	[g]	[g]	[°C]	[Mg/m³]	[Mg/m³]	[Mg/m³]	[%]
180	137.8	83.6	137.9	24.5	0.997	2.531	2.537	0.25
100	135.8	82.1	135.9	24.5	0.997	2.517	2.537	0.78
50	134.8	80.7	134.9	24.5	0.997	2.480	2.537	2.24
30	119.1	70.9	119.3	24.5	0.997	2.454	2.537	3.27

Table 6.3: Voids percentage in specimens at different compaction effort

6.3 Results and discussion

Three specimens are obtained using the same bituminous mixture but with different compaction effort. The three target gyrations used are 180, 100, 50 and 30. The voids percentage obtained for each specimen are summarized in Table 6.3.

Measurement to evaluate CTC and CTC are evaluated when the specimen is in thermal equilibrium in accordance with the first method. In Figure 6.5 are summarized the value of CTC and CTE obtained for each void's percentage.
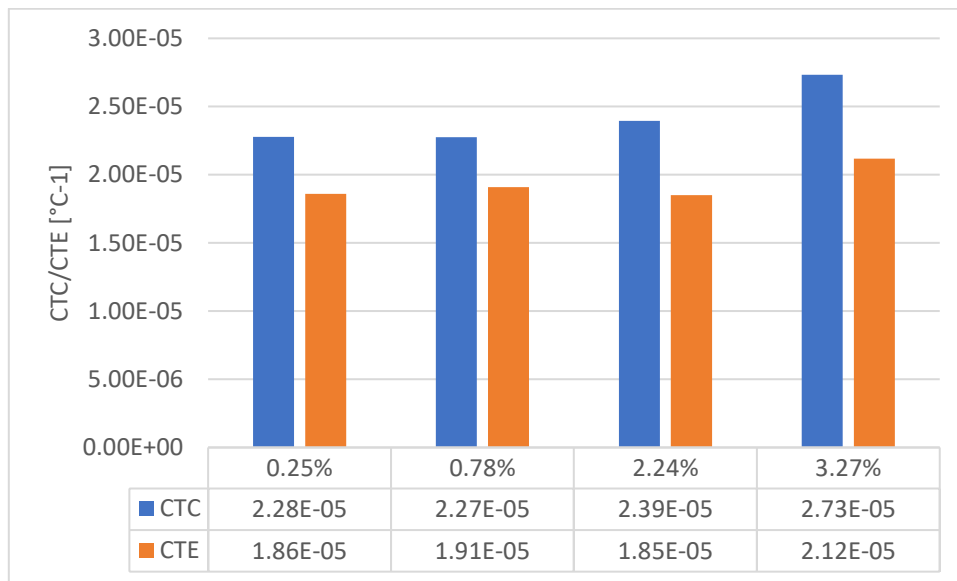

CTC/CTE [°C-1]	0.25%	0.78%	2.24%	3.27%
■ CTC	2.28E-05	2.27E-05	2.39E-05	2.73E-05
■ CTE	1.86E-05	1.91E-05	1.85E-05	2.12E-05

Figure 6.5: CTC and CTE at different voids percentage

CTC and CTE values are still comparable with those found in literature, more specifically CTC oscillates from $2.27 \times 10^{-5}\,°C^{-1}$ to $2.73 \times 10^{-5}\,°C^{-1}$, while CTE oscillates from $1.86 \times 10^{-5}\,°C^{-1}$ to $2.12 \times 10^{-5}\,°C^{-1}$.

For CTC values we observe that they increase with a direct proportional relationship to the void's percentage being very similar at 180 and 100 gyration and increasing at 50 and 30 gyrations.

CTE values in general are lower than CTC in accordance with the viscoelastic characteristic of asphalt concrete. CTE values are more regular between 180 and 50 gyrations while at 30 gyration we have a significant increase of CTE.

CHAPTER 7
CONCLUSION AND FURTHER
DEVELOPMENT

The thesis work aims to develop a new test method to evaluate the coefficient of thermal contraction and expansion of asphalt concrete. More specifically the test should be implemented to be as automatic as possible using the Dynamic Shear Rheometer (DSR). The DSR, normally used for rheology characterization of material, can indeed measure with great precision temperature and gap which are the input to evaluate CTC and CTE. Combining different DSR's accessorize of different standard setup a new instrumental configuration was created to test specimen of adequate dimension and to allow automatic gap measurements.

In the first approach the specimen's heights were measured only when thermal equilibrium is reached at four specific temperatures. A resting time at the target temperature should be provided to ensure thermal equilibrium through all the specimen's depth. On one hand this approach requires long time to be performed and give few information about specimen deformations, on the other hand the measuring system shows no thermal deformations. A different approach was developed trying to shorten the procedure and increasing the number of measurements acquired. The sample undergo a constant thermal ramp and heights' measurements are taken every ten second and hence the measuring system is constantly in contact with the sample. Performing the test without ensuring thermal equilibrium will induce some errors in the correct evaluation of CTC and CTE due to difference of temperature of the specimen and the measuring

cell. Moreover, the measuring system is affected by the change in temperature affecting the evaluation of the coefficients. Using benefits from the two previous approaches a third one was developed. To make the procedure as short as possible a constant gradient is used, and to better described deformations height's measurement are performed every 12 minutes and to prevent thermal deformations between two consecutive measurements the measuring system is kept outside the measuring cell.

Comparing the results obtained was found that the first approach is the one giving the best value and to validate it, measurement of material with known values of CTC were tested. The chosen material was: Ceramic, Invar36, Aluminium, Stainless steel. Their values were correctly predicted since they were comparable to those found in literature.

To evaluate the repeatability of the procedure a sample of Aluminium and was tested applying thermal. The results obtained showed no variation in the results confirming the repeatability of the procedure. Same procedure was performed on an asphalt concrete sample. In accordance with its viscoelastic behaviour was observed that deformation caused to a cooling ramp are not the same for a heating ramp. This leads to the evaluation of two different coefficient: coefficient of thermal contraction and coefficient of thermal expansion. Furthermore, cycle after cycle the value of CTC show the tendency to increase while CTE show the tendency to decrease meaning that CTC and CTE are dependent form their thermal history.

A practical application of the first method was proposed to evaluate how air voids affects CTC and CTE. Four different samples with different voids content were realized and tested. Was observed a direct proportionality between voids and CTE and CTC. Different investigation about how the mix characteristics affect the CTE and CTC should be performed such as bitumen content, aggregates nature and aggregates distribution. Also, how rheological properties of bitumen and its aging could influence CTC and CTE in order to built a mathematical model to predict CTC and CTE.

To conclude it is possible to affirm that the Method developed and implemented with the DSR is promising and able to give reliable results.

However, some improvement should be carried out. In place of the standard disposable measuring system it is possible to use a different material that shows low thermal contraction such as INVAR or ZERODUR®. In this way we are able to reduce environmental temperature influences.

A system to monitor the specimen's surface temperatures and specimen's core temperature could help to improve the efficiency of the test being able to test different bituminous mixture that could have different thermal equilibrium time.

REFERENCES

[1]   O. F. New, R. Pavement, F. Calibration, O. F. The, and T. Cracking, "Appendix Hh : Field Calibration of the Thermal Cracking," no. December, 2003.

[2]   R. a. Serway and J. W. Jewett, "Physics for Scientists and Engineers, Volume 1," p. 1215, 2007.

[3]   ASM, "NOTES CHECK REF Thermal Expansion," pp. 5–7, 2002.

[4]   J. D. James, J. A. Spittle, S. G. R. Brown, and R. W. Evans, "A review of measurement techniques for the thermal expansion coefficient of metals and alloys at elevated temperatures," *Meas. Sci. Technol.*, vol. 12, no. 3, pp. R1–R15, 2001.

[5]   ASTM E228, "Linear Thermal Expansion of Solid Materials With a Push-Rod Dilatometer," vol. i, pp. 1–10, 2011.

[6]   A. Standards, "E831 – 14:Standard Test Method for Linear Expansion of Solid Materials by Thermomechanical Analysis.," *ASTM Int.*, pp. 1–5, 2014.

[7]   American Society for Testing and Materials, "E289-04: Standard Test Method for Linear Thermal Expansion of Rigid Solids with Interferometry," vol. i, pp. 82–90, 2004.

[8]   M. Zeng and D. H. Shields, "Nonlinear thermal expansion and contraction of asphalt concrete," *Can. J. Civ. Eng.*, vol. 26, no. 1, pp. 26–34, 2011.

[9]   M. Mamlouk, M. Witczak, K. Kaloush, and N. Hasan, "Determination of Thermal Properties of Asphalt Mixtures," *J. Test. Eval.*, vol. 33, no. 2, p. 12592, 2005.

[10]   M. R. Islam and R. A. Tarefder, "Determining Coefficients of Thermal Contraction and Expansion of Asphalt Concrete Using Horizontal Asphalt Strain Gage," *Adv. Civ. Eng. Mater.*, vol. 3, no. 1, p. 20130101, 2014.

[11]   M. Akentuna, S. S. Kim, M. Nazzal, and A. R. Abbas, "Asphalt Mixture CTE

Measurement and the Determination of Factors Affecting CTE," *J. Mater. Civ. Eng.*, vol. 29, no. 6, p. 04017010, 2017.

[12] Y. A. Mehta, D. W. Chrislensen, and S. M. Stoffels, "Determination of Coefficient ofThermal Contraction of Asphalt Concrete Using Indirect Tensile Test Hardware Journal of Assoc / Q / lOn of Asphalt Paving Technologists," no. 814.

[13] M. R. Mitchell, R. E. Link, Q. Xu, and M. Solaimanian, "Measurement and Evaluation of Asphalt Concrete Thermal Expansion and Contraction," *J. Test. Eval.*, vol. 36, no. 2, p. 101024, 2007.